Molecular Phylogenetics and Evolution 56 (2010) 659–674

Contents lists available at ScienceDirect

Molecular Phylogenetics and Evolution

journal homepage: www.elsevier.com/locate/ympev

A multi-locus time-calibrated phylogeny of the brown algae (Heterokonta, Ochrophyta, Phaeophyceae): Investigating the evolutionary nature of the "brown algal crown radiation"

Thomas Silberfeld [a,*], Jessica W. Leigh [b], Heroen Verbruggen [c], Corinne Cruaud [d], Bruno de Reviers [a], Florence Rousseau [a]

[a] UMR 7138, UPMC, MNHN, CNRS, IRD: Systématique, adaptation, évolution, Département Systématique & évolution, USM 603, Muséum National d'Histoire Naturelle, 57 rue Cuvier, CP 39, 75231 Paris cedex 05, France
[b] UMR 7138, UPMC, MNHN, CNRS, IRD: Systématique, adaptation, évolution, Département Systématique & évolution, Université Pierre et Marie Curie, 7 quai Saint-Bernard, Bâtiment A, 4ème étage, 75005 Paris, France
[c] Phycology Research Group and Center for Molecular Phylogenetics and Evolution, Ghent University, Krijgslaan 281, Building S8, 9000 Ghent, Belgium
[d] Genoscope. Centre national de séquençage. 2, rue Gaston Crémieux, CP 5706, 91057 Evry cedex, France

ARTICLE INFO

Article history:
Received 26 November 2009
Revised 9 April 2010
Accepted 13 April 2010
Available online 19 April 2010

Keywords:
Phaeophyceae
Brown algal crown radiation
Multi-marker phylogeny
Time-calibrated phylogeny
Bayesian relaxed molecular clock
Hard/soft polytomy
Non-molecular characters evolution

ABSTRACT

The most conspicuous feature in previous phaeophycean phylogenies is a large polytomy known as the brown algal crown radiation (BACR). The BACR encompasses 10 out of the 17 currently recognized brown algal orders. A recent study has been able to resolve a few nodes of the BACR, suggesting that it may be a soft polytomy caused by a lack of signal in molecular markers. The present work aims to refine relationships within the BACR and investigate the nature and timeframe of the diversification in question using a dual approach. A multi-marker phylogeny of the brown algae was built from 10 mitochondrial, plastid and nuclear loci (>10,000 nt) of 72 phaeophycean taxa, resulting in trees with well-resolved inter-ordinal relationships within the BACR. Using Bayesian relaxed molecular clock analysis, it is shown that the BACR is likely to represent a gradual diversification spanning most of the Lower Cretaceous rather than a sudden radiation. Non-molecular characters classically used in ordinal delimitation were mapped on the molecular topology to study their evolutionary history.

1. Introduction

The brown algae or Phaeophyceae are a class of mostly marine macroalgae that are of particular evolutionary interest because they represent one of the four major lineages that have developed a complex multicellular organization (others being the Plantae, Fungi and Metazoa) (Charrier et al., 2008). All of the estimated 1811 species (Guiry and Guiry, 2010), belonging to *ca* 285 genera (Reviers et al., 2007), are multicellular. Several lineages have evolved differentiated and organized tissues, sometimes reminiscent of vascular or epidermal tissue, and can reach several meters in length. This is particularly obvious in kelp (order Laminariales) and wrack (order Fucales) species. A robust phylogenetic hypothesis is a prerequisite to formulate reliable evolutionary hypotheses on how and when characters related to the development of complex multicellularity evolved. Despite the progress made in circumscribing orders and reconstructing the shallower parts of the brown algal tree of life, most deep branches have proven difficult to resolve.

In traditional brown algal classifications, four features have been considered relevant at the ordinal level: the type of life history (isomorphic *versus* heteromorphic), the type of fertilization (isogamy, anisogamy, oogamy), the growth mode (terminal or intercalary, localized or diffuse) and the thallus architecture (haplostichous, polystichous, parenchymatous). An isomorphic life history, isogamous fertilization, and a haplostichous construction have been *a priori* considered as the most primitive states.

Abbreviations: *atp*9, mitochondrial ATP synthase subunit 9 gene; *atp*B, plastid ATP synthase subunit β gene; BACR, brown algal crown radiation; BI, Bayesian inference; BP, bootstrap proportion; *cox*1 (resp. *cox*3), cytochrome *c* oxidase subunit 1 (resp. 3) gene; cp, chloroplastic; ITS, internal transcribed spacer; LSU, large subunit of 28S rRNA gene; LTT, lineages through time; ML, maximum likelihood; mt, mitochondrial; *nad*1 (resp. *nad*4), NADH dehydrogenase subunit 1 (resp. 4) gene; nt, nucleotide(s); PP, Bayesian posterior probability; *rbc*L, large subunit of plastid encoded ribulose-1,5-biphosphate carboxylase oxygenase gene; *psa*A, photosystem I P700 chlorophyll *a* apoprotein A1 gene; *psb*A, photosystem II protein D1 gene; SSD(O), Sphacelariales–Syringodermatales–Dictyotales–(Onslowiales) lineage.

* Corresponding author.
E-mail address: silberfeld@mnhn.fr (T. Silberfeld).
URL: http://www.genoscope.fr (C. Cruaud).

1055-7903/$ - see front matter © 2010 Elsevier Inc. All rights reserved.
doi:10.1016/j.ympev.2010.04.020

The Ectocarpales, which display a combination of these three character states, were considered to be the earliest diverging brown algal lineage (Reviers and Rousseau, 1999 and references therein). All other lineages except the Fucales were considered to have evolved from an ectocarpalean ancestor that developed a digenetic haplodiplontic life cycle. Because of their peculiar life cycle, the Fucales were considered as an early diverging lineage that evolved independently for a long period of time (Wynne and Loiseaux, 1976).

The pioneer molecular phylogenetic studies of brown algae showed that the axiomatic primitive status of the Ectocarpales was wrong (Tan and Druehl, 1993, 1994, 1996). Later studies have reassessed the evolutionary relationships within the Phaeophyceae with increasingly comprehensive taxon and gene sampling. Studies of partial SSU and LSU rDNA and *rbc*L sequence data showed that the Dictyotales, Sphacelariales and Syringodermatales were early diverging lineages and that the remaining orders clustered in a poorly resolved polytomy that has become known as the brown algal crown radiation (BACR) (Reviers and Rousseau, 1999; Draisma et al., 2001; Rousseau et al., 2001). Subsequent work has mostly focused on identifying the earliest diverging phaeophycean taxa. The order Discosporangiales was shown to be the earliest-diverging order (Draisma et al., 2001; Kawai et al., 2007), followed by the Ishigeales (Cho et al., 2004) and the lineage comprising Dictyotales, Sphacelariales and Syringodermatales. Recent work shows that the Onslowiales cluster with the latter three orders, and the resulting lineage was named the SSDO clade (Draisma and Prud'homme Van Reine, 2001; Bittner et al., 2008; Phillips et al., 2008a). Other studies have focused on a lower taxonomic level: e.g. circumscribing limits of the Ectocarpales (Rousseau and Reviers, 1999; Peters and Ramírez, 2001), broadening of the concept of the Tilopteridales (Sasaki et al., 2001; Kawai and Sasaki, 2004), and unravelling the phylogenetic relationships within Fucales (Cho et al., 2006) and Laminariales (Yoon et al., 2001; Lane et al., 2006). However, despite the increasing number of molecular markers used throughout the last decade, none of these studies have managed to resolve phylogenetic relationships within the BACR, reinforcing the notion that it represents an episode of rapid diversification.

However, the recent study of Phillips et al. (2008a), based on global and local analyses of LSU rDNA and *rbc*L sequences for a broad selection of taxa suggested that at least part of the poor resolution of the BACR could be attributed to outgroup rooting artifacts and limitations of the molecular markers. Hence the possibility was raised that the BACR might not actually be a hard polytomy but an artifact of analyses based on too few molecular markers or markers uninformative about deep relationships (Phillips et al., 2008a). Despite the significant progress that has been made over the years, many uncertainties about the nature and branching order of the BACR remain. One of the main shortcomings in the recent studies is that none featured a combination of strong taxon and gene sampling, while the combination of both is obviously important in resolving rapid diversifications (Thomson and Shaffer, 2010; Geuten et al., 2007).

The primary goal of this study is to overcome this limitation by generating and analyzing a molecular dataset with strong taxon and gene sampling (72 taxa, 10 genes). First, we aim to refine relationships within the BACR using model-based phylogenetic inference with carefully selected composite models that take the various complexities of our multi-marker dataset into account. Second, we aim to gain insight into the nature and timeframe of the diversification of the BACR by inferring a time-calibrated class-level phylogeny of the brown algae and studying patterns of ordinal diversification through time. Third, we aim to improve current insights in the evolutionary history of brown algae by investigating the evolutionary history of the non-molecular characters that defined earlier taxonomic schemes.

2. Materials and methods

2.1. Taxon sampling

We selected 72 taxa representing ten orders of the brown algal crown radiation and three orders of the SSDO clade, out of the 17 currently recognized brown algal orders and including all ten orders of the BACR. With the exception of the monotypic orders Ascoseirales and Nemodermatales, BACR orders were represented by at least two taxa belonging to distinct genera. Since the present study focuses on relationships within the BACR, trees were rooted with members of Dictyotales (*Dictyopteris polypodioides*, *Dictyota dichotoma* and *Padina* spp.), Sphacelariales (*Cladostephus spongiosus*) and Syringodermatales (*Syringoderma phinneyi*). It has been demonstrated with confidence that these taxa cluster as the sister group to the BACR (Bittner et al., 2008). A list of taxa with voucher and DNA numbers and collection information is provided in Table 1. Voucher specimens were deposited in the Muséum National d'Histoire Naturelle of Paris (PC).

2.2. DNA extraction, amplification and sequencing

Total genomic DNA was extracted with a modified DNeasy Plant MiniKit protocol (Qiagen, Hilden, Germany), according to the brown algae specific protocol developed in Snirc et al. (2010). Sequences of the five mitochondrial genes *cox*1, *cox*3, *nad*1, *nad*4 and *atp*9, and of the four plastid genes *rbc*L, *psa*A, *psb*A and *atp*B, were amplified and sequenced. Primers were newly designed for the five mitochondrial genes *cox*1, *cox*3, *nad*1, *nad*4 and *atp*9 on the basis of the five published complete mitochondrial genomes of *Pylaiella littoralis* (Oudot-Le Secq et al., 2001), *Laminaria digitata* (Oudot-Le Secq et al., 2002), *Dictyota dichotoma*, *Fucus vesiculosus* and *Desmarestia viridis* (Oudot-Le Secq et al., 2006). Sequences of *cox*1 (1254 nt) were amplified as two overlapping fragments using the primer pairs *cox*1-117F/*cox*1-784R and *Gaz*F2/*Gaz*R2 for the first fragment and *cox*1-789F/*cox*1-1378R for the second fragment. Sequences of *cox*3 (693 nt), *nad*1 (780 nt), *nad*4 (738 nt) and *atp*9 (165 nt) were amplified as a single PCR product using the primer pairs *cox*3-44F/*cox*3-739R or *cox*3-67F/*cox*3-623R, *nad*1-113F/*nad*1-895R, *nad*4-242F/*nad*4-985R and *atp*9-22F/*atp*9-190R, respectively. Sequences of *rbc*L (1205 nt) and *psa*A (1400 nt) were amplified and sequenced as two overlapping fragments with the following primer pairs: *rbc*L-68F/*rbc*L-708R and *rbc*L-543F/*rbc*L-1381R for *rbc*L sequences, and *psa*A-130F/*psa*A-940R and *psa*A-870F/1760R for *psa*A sequences. *psb*A (903 nt) and *atp*B (608 nt) sequences were amplified as a single fragment using the *psb*A-F/*psb*A-R2 and *atp*B-Fb/*atp*B-2R primer pairs, respectively. All LSU (28S rDNA) sequences used in this study were taken from Phillips et al. (2008a). All primer sequences, annealing temperatures and, if necessary, bibliographical sources are listed in Table S1, provided as Supplementary material.

PCRs consisted of an initial denaturation step at 94 °C for 3 min, 35 cycles consisting of denaturation at 94 °C for 45 s, annealing at the temperatures given in Table S1 for 60 s, and elongation at 72 °C for between 60 and 90 s, depending of the length of the amplified fragment. The 35 cycles were followed by a final extension at 72 °C for 5 min. The resulting products were purified and used as matrix for cycle sequencing reaction with the same primers used for the PCR. Purification and cycle sequencing were performed by Genoscope (Évry, France). Raw sequences were edited and assembled with Sequencher™ 4.1 (Gene Codes Corporation, Ann Arbor, Michigan).

Table 1
Taxonomical list of the 72 taxa included in this study, with indication of the systematic position, herbarium and voucher ID, locality and date of collection, and identity of the collector.

Taxonomy	Herbarium ID	DNA No.	Locality and date of collection	Collector
Ascoseirales J. Petrov				
Ascoseiraceae Skottsberg				
Ascoseira mirabilis Skottsberg	–	FRA0145	Antarctic Penninsula (Antarctica) – 21.XII.1997	A. Peters
Desmarestiales Setchell *et* Gardner				
Arthrocladiaceae Chauvin				
Arthrocladia villosa (Hudson) Duby	PC0171167	FRA0122	Coutainville (Normandy, France) – VIII.1999	F. Rousseau
Desmarestiaceae (Thuret) Kjellman				
Desmarestia aculeata (L.) J.V. Lamouroux	PC0171168	FRA0497	St-Quay-Portrieux (Brittany, France) – 28.VIII.2004	T. Le Goff
Desmarestia ligulata (Lightfoot) J.V. Lamouroux	PC0171169	FRA0498	Trébeurden (Brittany, France) – 05.III.2004	T. Le Goff
Desmarestia menziesii J. Agardh	PC0171170	TJS0105	Dumont d'Urville (Terre Adélie, Antarctica) – 25.XII.2007	T. Silberfeld
Desmarestia viridis (O.F. Müller) J.V. Lamouroux	PC0171171	FRA0496	Trébeurden (Brittany, France) – V.2004	T. Le Goff
Himantothallus grandifolius (A. & E. Gepp) Zinova	PC0171172	TJS0099	Dumont d'Urville (Terre Adélie, Antarctica) – 25.XII.2007	T. Silberfeld
Dictyotales Bory de Saint-Vincent				
Dictyotaceae J.V. Lamouroux *ex* Dumortier				
Dictyopteris polypodioides (D.C.) J.V. Lamouroux	PC0171173	FRA0513	Sausset-les-Pins (Provence, France) – 23.VII.2006	T. Silberfeld
Dictyota dichotoma (Hudson) J.V. Lamouroux	PC0171174	FRA0512	Coutainville (Normandy, France) – VIII.1999	F. Rousseau
Padina pavonica (L.) Thivy	PC0171175	FRA0509	Ile des Embiez (Provence, France) – 26.VII.2006	T. Silberfeld
Ectocarpales Setchell *et* Gardner *s.l.*				
Acinetosporaceae G. Hamel *ex* J. Feldmann				
Hincksia granulosa (J.E. Smith) P.C. Silva	PC0171176	FRA0506	Ste-Honorine (Normandy, France) – 20.IX.2006	B. de Reviers
Pylaiella littoralis (L.) Kjellman	–	FRA0525	Roscoff (Brittany, France) – 12.III.2007	N. Simon
Chordariaceae Greville				
Asperococcus bullosus J.V. Lamouroux	PC0171177	FRA0499	St-Gast (Brittany, France) – 24.VI.2004	T. Le Goff
Elachista fucicola (Velley) J.E. Areschoug	PC0171178	FRA0501	Etretat (Normandy, France) – 30.IV.2006	T. Silberfeld
Leathesia difformis (L.) J.E. Areschoug	PC0171179	TJS0059	Plouguerneau (Brittany, France) – 15.VII.2007	T. Silberfeld
Punctaria latifolia Greville	PC0171180	FRA0503	Roscoff (Brittany, France) – 25.III.2005	T. Silberfeld
Ectocarpaceae C. Agardh				
Ectocarpus sp.	–	FRA0524	Roscoff (Brittany, France) – 12.III.2007	N. Simon
Petrospongiaceae M.-F.L.P. Racault et al.				
Petrospongium berkeleyi (Greville) Nägeli *ex* Kützing	PC0171181	FRA0294	Plouguerneau (Brittany, France) – 23.VII.2005	B. de Reviers
Scytosiphonaceae Ardissone *et* Straforello				
Chnoospora implexa J. Agardh	–	NC07-991	Port Boisé (New Caledonia) – 20.XI.2007	C.E. Payri
Colpomenia peregrina Sauvageau	PC0171182	FRA0505	Roscoff (Brittany, France) – 21.VII.2005	B. de Reviers
Hydroclathrus clathratus (C. Agardh) M.A. Howe	–	NC07-1001	Banc du Nord (New Caledonia) – 28.XI.2008	C.E. Payri
Petalonia fascia (O.F. Müller) Kuntze	PC0171183	FRA0504	Etretat (Normandy, France) – 20.IV.2006)	T. Silberfeld
Rosenvingea intricata (J. Agardh) Børgesen	–	NC07-996	Ricaudy (New Caledonia) – 27.XI.2008	C.E. Payri
Scytosiphon lomentaria (Lyngbye) Link	PC0171184	FRA0490	Plouguerneau (Brittany, France) – 25.III.2005	B. de Reviers
Fucales Bory de Saint-Vincent				
Durvillaeaceae (Oltmanns) De Toni				
Durvillaea potatorum (Labillardière) Areschoug	–	FRA0482	Blow Hole (Tas., Australia) – 06.X.2006	A. Millar
Fucaceae Adanson				
Ascophyllum nodosum (L.) Le Jolis	PC0171185	FRA0521	Roscoff (Brittany, France) – 29.III.2005	T. Silberfeld
Fucus vesiculosus L.	PC0171186	FRA0119	Roscoff (Brittany, France) – 06.X.1994	B. de Reviers
Pelvetia canaliculata (L.) Decaisne *et* Thuret	PC0171187	FRA0491	Roscoff (Brittany, France) – 25.III.2005	T. Silberfeld
Himanthaliaceae (Kjellman) De Toni				
Himanthalia elongata (L.) S.F. Gray	PC0171188	FRA0480	Roscoff (Brittany, France) – 21.VII.2005	B. de Reviers
Hormosiraceae Fritsch				
Hormosira banksii (Turner) Decaisne	–	FRA0483	Nelson's Lagoon (Vic., Australia) – 10.I.2007	A. Millar
Notheiaceae O.C. Schmidt				
Notheia anomala Harvey *et* Bailey	–	FRA0484	Lighthouse Reef (Vic., Australia) – 02.X.2006	N. Yee
Sargassaceae Kützing *s.l.*				
Bifurcaria bifurcata R. Ross	PC0171189	FRA0520	Roscoff (Brittany, France) – 22.III.2005	T. Silberfeld
Caulocystis cephalornithos (Labillardière) Areschoug	PC0171190	TJS0158	Taroona (Tas., Australia) – 28.I.2008	T. Silberfeld
Caulocystis uvifera (C. Agardh) Areschoug	PC0171191	TJS0182	Swansea (Tas., Australia) – 02.II.2008	T. Silberfeld
Cystophora grevillei (C. Agardh *ex* Sonder) J. Agardh	PC0171192	TJS0184	Swansea (Tas. Australia) – 02.II.2008	T. Silberfeld
Cystophora retorta (Mertens) J. Agardh	PC0171193	TJS0157	Taroona (Tas., Australia) – 28.I.2008	T. Silberfeld
Cystoseira baccata (S.G. Gmelin) P.C. Silva	PC0171194	FRA0487	Roscoff (Brittany, France) – 22.VII.2005	B. de Reviers
Cystoseira nodicaulis (Withering) M. Roberts	PC0171195	TJS0065	Roscoff (Brittany, France) – 16.VII.2007	N. Simon
Cystoseira tamariscifolia (Hudson) Papenfuss	PC0171196	FRA0492	Roscoff (Brittany, France) – 22.VII.2005	B. de Reviers
Halidrys siliquosa (L.) Lyngbye	PC0171197	TJS0057	Roscoff (Brittany, France) – 14.VII.2007	W. Kooistra
Sargassum fallax Sonder	PC0171198	TJS0168	Eaglehawk Neck (Tas. Australia) – 31.XII.2007	T. Silberfeld
Sargassum muticum (Yendo) Fensholt	PC0171199	FRA0486	Roscoff (Brittany, France) – 21.VII.2005	B. de Reviers
Seirococcaceae Nizamuddin				
Phyllospora comosa (Labillardière) C. Agardh	–	FRA0485	Lighthouse Reef (Vic., Australia) – 02.X.2006	A. Millar
Seirococcus axillaris (Brown *ex* Turner) Greville	–	FRA0065	Beachport (S.A., Australia) – 20.II.1997	Wm. J. Woelkerling
Xiphophoraceae G.Y. Cho, F. Rousseau, B. de Reviers *et* S.M. Boo				
Xiphophora chondrophylla (Brown *ex* Turner) Montagne *ex* Harvey	–	FRA0063	Flinders (Vic., Australia) – II.1997	Wm. J. Woelkerling

(*continued on next page*)

Table 1 (*continued*)

Taxonomy	Herbarium ID	DNA No.	Locality and date of collection	Collector
***Incertae sedis* at ordinal rank**				
Bachelotia antillarum (Grunow) Gerloff	–	FRA0100	Cultured strain	A. Peters
Laminariales Migula				
Alariaceae Setchell *et* Gardner				
Alaria esculenta (L.) Greville	PC0171200	TJS0041	Ile de Batz (Brittany, France) – 14.VII.2007	T. Silberfeld
Undaria pinnatifida (Harvey) Suringar	PC0171201	LLG0138	Rio dei Greci (Venezia, Italia) – 15.V.2005	L. Le Gall
Chordaceae Dumortier				
Chorda filum (L.) Stackhouse	PC0171202	FRA0481	Bréhec (Brittany, France) – 19.VI.2004	T. Le Goff
Costariaceae C.E. Lane, C. Mayes, Druehl *et* G.W. Saunders				
Agarum clathratum Dumortier	PC0171203	LLG0013	Louisebourg (Nova Scotia, Canada) – 30.VIII.2004	L. Le Gall
Laminariaceae Bory de Saint-Vincent				
Laminaria digitata (Hudson) J.V. Lamouroux	PC0171204	FRA0082	Roscoff (Brittany, France) – 04.12.1996	B. de Reviers
Nereocystis luetkeana (K. Mertens) Postels *et* Ruprecht	–	–	*Genbank data only*	–
Pelagophycus porra (Léman) Setchell	–	–	*Genbank data only*	–
Saccharina latissima (L.) Lane, Mayes, Druehl *et* Saunders	PC0171205	FRA0508	Roscoff (Brittany, France) – 21.VII.2005	B. de Reviers
Lessoniaceae Setchell *et* Gardner				
Ecklonia radiata (C. Agardh) J. Agardh	PC0171206	TJS0152	Taroona (Tas., Australia) – 28.I.2008	T. Silberfeld
Nemodermatales M. Parente, R.L. Fletcher, F. Rousseau *et* N. Phillips				
Nemodermataceae Kuckuck *ex* Feldmann				
Nemoderma tingitanum Shousboe *ex* Bornet	PC0171207	FRA0530	Banyuls (Roussillon, France) – VII.2004	F. Rousseau
Ralfsiales Nakamura *ex* Lim *et* Kawai				
Ralfsiaceae Farlow				
Analipus japonicus (Harvey) M.J. Wynne	–	BH-08-10	Bodega Bay (CA, USA) – 03.VII.2008	K. Miller, R. Moe
Ralfsia fungiformis (Gunnerus) Setchell *et* Gardner	PC0171208	FRA0187	Cap du Bon Désir (QC, Canada) – 21.III.2004	L. Le Gall
Scytothamnales A.F. Peters *et* M.N. Clayton				
Scytothamnaceae Setchell *et* Gardner				
Scytothamnus australis (J. Agardh) Hooker *et* Harvey	–	FRA0085	New Zealand – 23.IV.1997	W. Nelson
Splachnidiaceae Mitchell *et* Whitting				
Splachnidium rugosum (L.) Greville	PC0171209	FRA0086	Muyzemberg (South Africa) – 15.VIII.1996	O. Dargent
Sphacelariales Migula				
Sphacelariaceae Decaisne				
Cladostephus spongiosus (Hudson) C. Agardh	PC0171210	FRA0511	St-Quay-Portrieux (Brittany, France) – 28.VIII.2005	T. Silberfeld
Sporochnales Sauvageau				
Sporochnaceae Greville				
Bellotia eriophorum Harvey	PC0171211	TJS0128	Taroona (Tas., Australia) – 28.I.2008	T. Silberfeld
Carpomitra costata (Stackhouse) Batters	–	NY045	Bruny Island (Tas., Australia) – 01.XII.2002	N. Yee
Perithalia caudata J. Agardh	–	NY046	Bruny Island (Tas., Australia) – 01.XII.2002	N. Yee
Sporochnus pedunculatus (Hudson) C. Agardh	PC0171212	FRA0494	St-Quay-Portrieux (Brittany, France) – 13.VI.2004	T. Le Goff
Syringodermatales E.C. Henry				
Syringodermataceae E.C. Henry				
Syringoderma phinneyi E.C. Henry *et* D.G. Müller	–	FRA0140	Cultured strain	A. Peters
Tilopteridales Bessey *s.l.*				
Cutleriaceae Griffith *et* Henfrey				
Cutleria multifida (Turner) Greville	PC0171213	FRA0479	Roscoff (Brittany, France) – 03.IX.1996	F. Rousseau
Zanardinia typus (Nardo) P.C. Silva	PC0171214	FRA0115	Aiguafreda (Catalunya, Spain) – date unknown	C. Rodríguez-Prieto
Phyllariaceae Tilden				
Phyllariopsis brevipes (C. Agardh) E.C. Henry *et* G.R. South	PC0171215	LLG2142	Port-Cros (Provence, France) – X.2008	L. Le Gall
Saccorhiza dermatodea (Bachelot de la Pylaie) Areschoug	–	FRA0144	Newfoundland (Canada) – 06.IV.2000	D.G. Müller
Saccorhiza polyschides (Lightfoot) Batters	PC0171216	FRA0478	Roscoff (Brittany, France) – 27.IX.1995	B. de Reviers
Tilopteridaceae Kjellman				
Tilopteris mertensii (Turner) Kützing	–	FRA0109	Cultured strain	A. Peters

2.3. Alignment generation

The 429 newly generated sequences and 149 downloaded from Genbank were aligned visually for each gene separately using the software MEGA version 4.0 (Tamura et al., 2007). Ambiguous regions of the LSU rDNA alignment, characterized by a high rate of insertion/deletion, were removed before analyses. All alignments are available from TreeBase (URL: http://purl.org/phylo/treebase/phylows/study/TB2:S10363) and www.phycoweb.net.

We focused our work on a 10325 nt long alignment, obtained by concatenation of the sequences of all markers for the 72 sampled taxa, and subsequently referred to as "complete data set" despite the occurrence of missing data (Table 2). Various subalignments were constructed: mitochondrial (mt: 3630 nt), plastid (cp: 4116 nt), organellar (cp + mt: 7746 nt) datasets, and their combinations with LSU data (mt + LSU: 6209 nt, and cp + LSU: 6695 nt). Mutational saturation was evaluated for first, second and third positions of mitochondrial and plastid subsets by plotting the GTR-corrected pairwise distance values against the uncorrected pairwise distance values (calculated with PAUP* version 4.0b10; Swofford, 1999).

2.4. Model testing and phylogenetic analyses

2.4.1. Evaluation of data congruence

Due to the presence of missing data in our alignments, the ILD test (Farris et al., 1994) and partitioned likelihood support (Lee and Hugall, 2003) cannot be used to evaluate data congruence. Instead, we performed a software-assisted evaluation of topological congruence of gene alignments with Concaterpillar version 1.4 (Leigh et al., 2008).

Table 2
Alphabetical list of species with Genbank accession numbers or source of the 578 sequences used in this study. Accession numbers of sequences obtained in this study are written in bold letters. Missing sequences are designed by a dash.

Taxon	*cox*1	*cox*3	*nad*1	*nad*4	*atp*9	*rbc*L	*psa*A	*psb*A	*atp*B	LSU
Agarum clathratum	**GQ368254**	**GQ368269**	**GQ368283**	–	**GQ368297**	**GQ368312**	**GQ368326**	**GQ368341**	**GQ368355**	AY851521
Alaria esculenta[a]	**EU681388**	**EU681431**	**EU681471**	**EU681515**	**EU681544**	**EU681587**	**EU681602**	**EU681624**	**EU681665**	AY851525[b] *A. marginata*
Analipus japonicus	**EU681389**	**EU681432**	**EU681472**	**EU681516**	**EU681545**	**EU681588**	AY372966	**EU681625**	–	–
Arthrocladia villosa	–	–	–	–	–	**EU681589**	**EU681603**	–	–	–
Ascophyllum nodosum	**EU681390**	**EU681433**	**EU681473**	**EU681517**	**EU681546**	AJ287853	AY372959	**EU681626**	**EU681666**	–
Ascoseira mirabilis	**EU681391**	–	**EU681474**	–	**EU681547**	EF990237	**EU681604**	**EU681627**	**EU681667**	EF990192
Asperococcus bullosus	**EU681392**	**EU681434**	**EU681475**	**EU681518**	**EU681548**	**EU681590**	**EU681605**	**EU681628**	**EU681668**	–
Bachelotia antillarum	**EU681393**	**EU681435**	**EU681476**	–	–	AF207797	EU579881	**EU681629**	**EU681669**	EF990236
Bellotia eriophorum	**GQ368255**	**GQ368270**	**GQ368284**	–	**GQ368298**	**GQ368313**	**GQ368327**	**GQ368342**	–	–
Bifurcaria bifurcata	**EU681394**	**EU681436**	**EU681477**	–	**EU681549**	AY590500	DQ092448	**EU681630**	**EU681670**	EF990215
Carpomitra costata	–	**EU681437**	**EU681478**	–	–	**EU681591**	**EU681606**	–	–	–
Caulocystis cephalornithos	**GQ368256**	**GQ368271**	**GQ368285**	–	**GQ368299**	**GQ368314**	**GQ368328**	**GQ368343**	–	–
Caulocystis uvifera	**GQ368257**	**GQ368272**	**GQ368286**	–	**GQ368300**	**GQ368315**	**GQ368329**	**GQ368344**	–	–
Chnoospora implexa	**GQ368258**	**GQ368273**	**GQ368287**	–	**GQ368301**	**GQ368316**	**GQ368330**	**GQ368345**	**GQ368356**	–
Chorda filum	–	**EU681438**	**EU681479**	–	**EU681550**	AY372983	AY372963	AY528848	**EU681671**	AY851505
Cladostephus spongiosus	**EU681396**	–	–	**EU681520**	–	AJ287863	EU579889	–	**EU681672**	EF990225
Colpomenia peregrina	**EU681397**	**EU681439**	**EU681481**	**EU681521**	**EU681552**	AB022235	DQ239776	**EU681631**	**EU681673**	–
Cutleria multifida[a]	**EU681398**	**EU681440**	**EU681482**	**EU681522**	**EU681553**	AY157692	AY372955[b] *C. cylindrica*	**EU681632**	**EU681674**	EF990231
Cystophora grevillei	–	**GQ368274**	**GQ368288**	–	**GQ368302**	**GQ368317**	**GQ368331**	**GQ368346**	**GQ368357**	–
Cystophora retorta	**GQ368259**	**GQ368275**	**GQ368289**	–	**GQ368303**	–	**GQ368332**	–	**GQ368358**	–
Cystoseira baccata	**EU681399**	**EU681441**	**EU681483**	–	**EU681554**	**EU681592**	**EU681607**	**EU681633**	**EU681675**	–
Cystoseira nodicaulis	**EU681400**	**EU681442**	**EU681484**	–	**EU681555**	**EU681593**	**EU681608**	**EU681634**	**EU681676**	–
Cystoseira tamariscifolia	**EU681401**	**EU681443**	**EU681485**	–	**EU681556**	**EU681594**	**EU681609**	**EU681635**	**EU681677**	–
Desmarestia aculeata	**EU681402**	–	**EU681486**	**EU681523**	**EU681557**	AJ287847	EU579882	**EU681636**	**EU681678**	EF990204
Desmarestia ligulata	**EU681403**	**EU681444**	**EU681487**	**EU681524**	**EU681558**	AJ287848	**EU681610**	**EU681637**	**EU681679**	–
Desmarestia menziesii	**GQ368260**	**GQ368276**	**GQ368290**	–	**GQ368304**	**GQ368318**	**GQ368333**	**GQ368347**	**GQ368359**	–
Desmarestia viridis	AY500367	AY500367	AY500367	AY500367	AY500367	AJ287849	**EU681611**	**EU681638**	**EU681680**	–
Dictyopteris polypodioides	**EU681404**	**EU681445**	–	**EU681525**	–	DQ472042	EU579899	**EU681639**	**EU681681**	–
Dictyota dichotoma	AY500368	AY500368	AY500368	AY500368	AY500368	DQ472051	AY422578	AY748321	X66939	AF331152
Durvillaea potatorum[a]	**EU681405**	**EU681446**	**EU681488**	**EU681526**	**EU681559**	EF990242	DQ092453[b] *D. antarctica*	**EU681640**	**EU681682**	EF990207
Ecklonia radiata	**GQ368261**	**GQ368277**	**GQ368291**	–	**GQ368305**	**GQ368319**	**GQ368334**	**GQ368348**	**GQ368360**	–
Ectocarpus sp.[a]	**EU681406**	**EU681447**	**EU681489**	**EU681527**	**EU681560**	AY372978	AY372949	X56695[b] *E. siliculosus*	**EU681683**	EF990201[b] *E. siliculosus*
Elachista fucicola	**EU681407**	**EU681448**	**EU681490**	–	**EU681561**	AF055398	**EU681612**	**EU681641**	**EU681684**	–
Fucus vesiculosus	AY494079	AY494079	AY494079	AY494079	AY494079	DQ307680	AY372960	**EU681642**	DQ307681	AF331151
Halidrys siliquosa	**EU681408**	**EU681449**	**EU681491**	–	**EU681562**	**EU681595**	**EU681613**	**EU681643**	**EU681685**	–
Himanthalia elongata	**EU681409**	**EU681450**	**EU681492**	–	**EU681563**	EF990246	DQ092459	**EU681644**	**EU681686**	EF990212
Himantothallus grandifolius	**GQ368262**	**GQ368278**	**GQ368292**	–	**GQ368306**	**GQ368320**	**GQ368335**	**GQ368349**	**GQ368361**	EF990206
Hincksia granulosa	**EU681410**	**EU681451**	**EU681493**	**EU681528**	**EU681564**	**EU681596**	**EU681614**	**EU681645**	**EU681687**	–
Hormosira banksii	**EU681411**	**EU681452**	**EU681494**	–	**EU681565**	EF990247	DQ092460	–	–	EF990213
Hydroclathrus clathratus	**GQ368263**	–	–	–	**GQ368307**	**GQ368321**	**GQ368336**	**GQ368350**	**GQ368362**	–
Laminaria digitata	AJ344328	AJ344328	AJ344328	AJ344328	AJ344328	AY851559	AY372964	**EU681646**	**EU681688**	AF331153
Leathesia difformis	**EU681412**	**EU681453**	**EU681495**	**EU681529**	**EU681566**	AY996365	AY996371	**EU681647**	–	–
Nemoderma tingitanum	–	–	**EU681496**	**EU681530**	**EU681567**	EF990253	DQ094835	–	**EU681689**	EF990221
Nereocystis luetkeana	FJ409182	–	AY862410	–	–	DQ372565	DQ372549	–	–	AY851509
Notheia anomala	**EU681413**	–	**EU681497**	–	**EU681568**	EF990248	DQ094837	**EU681648**	–	EF990214
Padina pavonica[a]	–	**EU681454**	**EU681498**	**EU681531**	**EU681569**	EU579961	EU579919	**EU681649**	**EU681690**	EF990195[b] *P. melemele*
Pelagophycus porra	EF218849	–	–	–	–	AJ287858	DQ473542	–	–	AY851508
Pelvetia canaliculata	**EU681414**	**EU681455**	**EU681499**	**EU681532**	**EU681570**	**EU681597**	**EU681615**	**EU681650**	**EU681691**	EF990210
Perithalia caudata	–	–	**EU681500**	–	–	**EU681598**	**EU681616**	–	–	–
Petalonia fascia	**EU681415**	**EU681456**	**EU681501**	**EU681533**	**EU681571**	AB022243	AY372953	**EU681651**	**EU681692**	EF990202
Petrospongium berkeleyi	**EU681416**	**EU681457**	**EU681502**	**EU681534**	**EU681572**	EU850275	EU850280	**EU681652**	**EU681693**	–
Phyllariopsis brevipes	**GQ368264**	**GQ368279**	**GQ368293**	–	**GQ368308**	**GQ368322**	**GQ368337**	**GQ368351**	**GQ368363**	–
Phyllospora comosa	**EU681417**	**EU681458**	**EU681503**	**EU681535**	**EU681573**	EF990249	**EU681617**	**EU681653**	–	EF990219
Punctaria latifolia	**EU681418**	**EU681459**	**EU681504**	**EU681536**	**EU681574**	AY095322	AY372948	**EU681654**	**EU681694**	–
Pylaiella littoralis	AJ277126	AJ277126	AJ277126	AJ277126	AJ277126	X55372	AY119724	AY119760	**EU681695**	EF990198
Ralfsia fungiformis	**EU681419**	**EU681460**	–	**EU681537**	**EU681575**	EU579936	EU579885	**EU681655**	**EU681696**	–
Rosenvingea intricata	**GQ368265**	**GQ368280**	**GQ368294**	–	**GQ368309**	**GQ368323**	**GQ368338**	**GQ368352**	**GQ368364**	–
Saccharina latissima	**EU681420**	–	**EU681505**	–	–	AY85156	**EU681618**	**EU681656**	**EU681697**	–
Saccorhiza dermatodea	**EU681421**	**EU681461**	**EU681506**	**EU681538**	**EU681576**	AB045252	**EU681619**	**EU681657**	**EU681698**	–
Saccorhiza polyschides	**EU681422**	**EU681462**	**EU681507**	**EU681539**	**EU681577**	AB045256	AY372965	**EU681658**	**EU681699**	EF990232
Sargassum fallax	**GQ368266**	**GQ368281**	**GQ368295**	–	**GQ368310**	**GQ368324**	**GQ368339**	**GQ368353**	–	–
Sargassum muticum	**EU681423**	**EU681463**	**EU681508**	–	**EU681578**	AJ287854	DQ092463	**EU681659**	**EU681700**	EF990218
Scytosiphon lomentaria	**EU681424**	**EU681464**	**EU681509**	**EU681540**	**EU681579**	AB022238	AY372954	**EU681660**	**EU681701**	EF990203
Scytothamnus australis	**EU681425**	–	–	**EU681541**	**EU681580**	AJ295833	AY372967	**EU681661**	**EU681702**	EF990223
Seirococcus axillaris	**EU681426**	–	**EU681510**	–	**EU681581**	**EU681599**	**EU681620**	**EU681662**	**EU681703**	–
Splachnidium rugosum	**EU681427**	**EU681465**	–	–	**EU681582**	AJ295834	AY372968	AY528853	**EU681704**	EF990224
Sporochnus pedunculatus	**EU681428**	**EU681466**	**EU681511**	**EU681542**	**EU681583**	EU579937	**EU681621**	**EU681663**	**EU681705**	EF990229
Syringoderma phinneyi	**EU681429**	**EU681467**	**EU681512**	**EU681543**	–	AJ287868	AY528862	AY528858	–	EF990230

(*continued on next page*)

Table 2 (*continued*)

Taxon	*cox*1	*cox*3	*nad*1	*nad*4	*atp*9	*rbc*L	*psa*A	*psb*A	*atp*B	LSU
Tilopteris mertensii	**EU681430**	**EU681468**	–	–	**EU681584**	AB045260	**EU681622**	–	**EU681706**	EF990234
Undaria pinnatifida	**GQ368267**	**GQ368282**	**GQ368296**	–	**GQ368311**	**GQ368325**	**GQ368340**	**GQ368354**	**GQ368366**	–
Xiphophora chondrophylla	**GQ368268**	**EU681469**	**EU681513**	–	**EU681585**	**EU681600**	DQ314586	–	**EU681707**	EF990220
Zanardinia typus	–	**EU681470**	**EU681514**	–	**EU681586**	**EU681601**	**EU681623**	**EU681664**	**EU681708**	–

[a] Indicates taxa for which at least one of the ten sequences belongs to another species of the considered genus.
[b] Indicates sequences belonging to another species of the considered genus. The corresponding species is thus indicated below the accession number.

2.4.2. Model testing and phylogenetic analyses

An appropriate partitioning scheme was chosen by applying a partitioned model selection pipeline that uses the Akaike Information Criterion (AIC, Akaike, 1974), second-order corrected AIC (AIC_C, Hurvich and Tsai, 1989), Bayesian Information Criterion (BIC, Schwarz, 1978), and Likelihood-Ratio Test (LRT, Huelsenbeck and Rannala, 1997). The tests were applied to assess whether GTR model parameters, proportion of invariant sites, the shape parameter for Γ-distributed rates across sites, and branch lengths should be estimated separately for each gene, each codon position, or both genes and codon positions. A diagram of hierarchical comparisons is provided as Supplementary material (Fig. S1). The preferred model was that in which the data set was partitioned by gene, and by codon position within protein-coding genes (i.e. 28 partition sections for the complete data set). Substitution model parameters were estimated separately for partitions, but branch lengths were shared among them. Model comparison detail for the complete data set is summarized in Table S2. The 28-partition GTR + I + Γ model was used for further phylogenetic analysis.

Maximum likelihood phylogenies were estimated using RA×ML (Stamatakis, 2006) with the GTR model and Γ-distributed rates across sites and an estimated proportion of invariant sites (Rodriguez et al., 1990). Data sets were partitioned and model parameters were estimated separately for different partitions. Maximum likelihood bootstrap analyses (Felsenstein, 1985) consisted of 1000 replicates.

The complete dataset was also analysed by Bayesian inference using MrBayes v.3.1.2. (Huelsenbeck and Ronquist, 2001; Ronquist and Huelsenbeck, 2003) with the same partitioned model. Analyses were performed as two independent runs, each with four incrementally heated Metropolis-coupled Monte-Carlo Markov Chains running for four million generations. Output trees and data were sampled every 100 generations. Likelihood values reached a plateau within 400,000 generations in all analyses. The first 400,000 generations were deleted as burn-in and a consensus tree was generated from the post-burn-in trees of both runs. In interpreting our trees, nodes will be considered "fully supported" if they have a ML bootstrap value (BP) of 100% and a Bayesian posterior probability value of 1.00, "strongly supported" for BP $\geqslant$ 85% and PP $\geqslant$ 0.95, "moderately supported" for 75% $\leqslant$ BP < 85% and 0.90 $\leqslant$ PP < 0.95, and "poorly supported" for BP < 75% and PP < 0.90%.

2.5. Relaxed molecular clock analysis

In order to provide a provisional estimate of the geological timeframe of brown algal diversification, including an age estimate of the BACR, and to investigate how much time it took for the various BACR lineages to diverge from each other, we inferred a time-calibrated brown algal phylogeny using a relaxed molecular clock method implemented in BEAST v.1.5.3 (Drummond and Rambaut, 2007). We specified the same 28 partitions as above with unlinked GTR + I + Γ models, an uncorrelated (lognormal) clock model and a Yule tree prior. Markov chains started from a tree obtained in a preliminary BEAST analysis and were run for 10 million generations, sampled every 1000th generation. The five outgroup taxa were forced to form a monophyletic group. Three other taxon groups were used as calibration points and we specified a prior on the root age – these settings are explained in detail below. Ten independent MCMC runs were carried out. Convergence of *ln*L and parameter values was monitored with Tracer v.1.4.1., and a burn-in value of two million generations was determined (Rambaut and Drummond, 2009). A maximum clade credibility chronogram with mean node heights was calculated from the post-burn-in set of trees with TreeAnnotator v.1.5.2. (Fig. 2). The consensus chronogram was based on the two chains that converged to the highest observed likelihood plateau. The other eight chains converged on suboptimal likelihood plateaus.

Three nodes in the tree were constrained in geological time based on knowledge from the fossil record and prior molecular clock analyses. Because brown algae have only soft tissues, they lack a consistent fossil record through time. A few Palaeozoic fossils have been assigned to *Dictyota*- or *Fucus*-like taxa because of their somewhat dichotomized ribbon shape (e.g. *Miaohephyton*, Xiao et al., 1998; *Perissothallus*, Krings et al., 2007), but these identifications are highly doubtful as such a shape also occurs in a variety of other lineages (see Section 4.3). In our opinion, only two geological formations have yielded fossils that can be confidently attributed to brown algae and used to constrain our relaxed molecular clock analysis.

(i) The Early Cretaceous (145.5–99.6 Ma) clay shales from the Gangapur formation (Andhra Pradesh state, India) yielded a fossil macroalga that reminds of extant species of the genus *Padina* Adanson (Rajanikanth, 1989). Although the note provides relatively little information in terms of accurate chronological or micro-structural data, the macroscopic examination of the sample, as well as the fact that *Padina* is one of the only two brown algal genera that precipitate $CaCO_3$ in their fronds (the other being the dictyotalean genus *Newhousia* Kraft, Saunders, Abbott *et* Haroun), led us to use this fossil as a calibration point. Thus, the occurrence of a *Padina*-like morphology in Early Cretaceous deposits was used to define a lower boundary at 99.6 Ma (end of Lower Cretaceous period) for the stem node of *Padina*.

(ii) The Miocene deposits (13–17 Ma) of the Monterey formation in California are also worth considering within our framework (Parker and Dawson, 1965). These fossil-rich diatomites yielded numerous exceptionally preserved fossils of soft green, red and brown algae some of which can be used to calibrate nodes in our analyses. Four species belonging to the genera *Paleocystophora* (*P. subopposita*) and *Paleohalidrys* (*P. californica*, *P. superba* and *P. occidentalis*) can be confidently assigned to the Fucalean family Sargassaceae because of their sympodial branching pattern. However, it is difficult to assign these fossils to extant genera, hence we decided to define a lower boundary at 13 Ma for the stem node of the Sargassaceae. Additionally, the fossil *Julescraneia grandicornis*, which has a branching pattern reminiscent of the extant laminarialean genera *Nereocystis* and *Pelagophycus*, was used to define a lower boundary at 13 Ma for the stem node of the *Nereocystis–Pelagophycus* clade.

These three calibrations were incorporated into the analysis by defining a uniform prior with a maximum age limit of 155 Ma and a minimum of 13 Ma for the Miocene fossils and 99.6 Ma for the fossil *Padina*. Finally, we defined a prior on the root age

of our tree based on the results of a previous molecular clock study. Medlin et al. (1997) performed molecular dating analyses for a broad selection of photosynthetic heterokonts. Although this study analysed the data under a strict molecular clock model, it was calibrated with the diatoms, a group with a very rich fossil record. This study estimated the earliest probable origin of the Phaeophyceae at *ca* 155 Ma. We therefore, applied an age prior on the root of our tree sampled from a normal distribution with mean of 155 Ma and standard deviation of 30 Ma. This prior is sufficiently informative to place a reasonable upper bound on the molecular clock while the standard deviation is broad enough to reflect the uncertainty about the calibration and permits the other three calibrations to determine posterior node ages (Sanders and Lee, 2007).

The obtained chronogram was used to construct a lineage-through-time (LTT) plot according to Harvey et al. (1994). This dot-plot, displaying the logarithm of the cumulative number of lineages occurring through time, allows further characterization of the pattern and tempo of diversification by providing a visual estimate of the variations of diversification rates through time (Harvey et al., 1994).

2.6. Evolution of non-molecular characters

The evolution and ancestral states of six morpho-anatomical and life-history characters were estimated with maximum likelihood methods. We used ML inference because this permits a probabilistic assessment of ancestral character states, taking branch lengths into account. We used the chronogram from the BEAST analysis as a reference tree because in this tree, branch lengths are proportional to evolutionary time. The states of the six morpho-anatomical and life-history characters in question were encoded for all taxa in our tree as specified in Supplementary Table S3. We were unable to score all taxa for characters A (life history) and B (type of fertilization). Character A was not scored for *Elachista fucicola*, *Petrospongium berkeleyi*, *Ralfsia fungiformis*, *Rosenvingea intricata* and *Tilopteris mertensii*, for which life history is unknown or asexual. Reproductive strategy was not scored for *Elachista fucicola*, *Petrospongium berkeleyi*, *Ralfsia fungiformis* and *Rosenvingea intricata*, for which only an asexual life history is known, and for *Bachelotia antillarum* for which the strategy could not be retrieved. Further details are provided as footnotes in Table S3.

Maximum likelihood inference of trait evolution was carried out with BayesTraits (Pagel and Meade, 2006). Analyses used the multistate model and assumed equal rates of change between all states. We opted for this option because it approaches maximum parsimony ancestral state reconstruction but allows probabilistic inferences and takes branch lengths into account. Moreover, it reduces the number of estimated model parameters. This choice is further discussed in Section 4.4. One thousand ML optimizations were carried out to avoid local optima. Ancestral state probabilities were obtained by specifying all internal nodes with a series of 'addnode' commands. The results of the ancestral character state estimations (i.e. the probabilities of different character states at each node) were plotted onto the chronogram with TreeGradients v.1.04 (Verbruggen, 2010). This program plots character state probabilities as colors along a color gradient, allowing intuitive visual assessment of the evolution of a character and of uncertainties that may exist at internal nodes.

3. Results

3.1. Data set properties and molecular evolution

3.1.1. Basic properties

No indels were detected in the protein-coding sequences, with the exception of a single codon deletion in the *cox*1 sequence of *Cladostephus spongiosus*. The combined mitochondrial data set has a smaller proportion of constant sites than the plastid data set (45.4% against 59.4%), whereas the LSU data exhibit a noticeably high percentage of constant sites (80.5%), which can in part be explained by the fact that ambiguous regions of the LSU alignment were discarded before analysis. Mitochondrial data are also more parsimony-informative than plastid data (45.6% against 33.6% of parsimony informative sites). Finally, 67.9% of the mitochondrial variable sites are third codon positions, whereas this is 78.6% for plastid data. Mitochondrial genes show more substitutional saturation than plastid genes (Fig. S2).

3.1.2. Congruence and concatenation of data sets

To assess the possible discrepancies between phylogenetic signals brought by each gene, we used Concaterpillar to identify mutually incongruent subsets of markers. Concaterpillar recovered four subsets, but the genes were not divided according to their genome of origin; instead, *atp*9 and *rbc*L were found to be incongruent with all other genes, while *cox*1 and *cox*3 formed one congruent subset, and the remaining genes a fourth. We performed RA×ML phylogenetic analyses of each of these congruent subsets individually, but because visual examination of the trees inferred from subsets indicates that (i) positions of only a few taxa vary between trees, and (ii) these taxa originate from poorly supported conflicting nodes (BP < 75%), we chose to infer a phylogeny from the complete dataset in addition to the congruent subsets. The trees produced by the analyses of the four subsets are provided as Supplementary material (Figs. S3, S4, S5 and S6).

3.2. Phylogenetic relationships

The topologies obtained in maximum likelihood and Bayesian inference on the complete data set were congruent at the inter-ordinal level. We chose to present the ML topology and label each node with its ML bootstrap and Bayesian posterior probability values (Fig. 1). All non-monotypic orders represented by more than one taxon of specific rank in our taxon sampling were found mono-

Fig. 1. ML phylogram resulting from the combined global data set (72 taxa, 10 genes, 10325 nt). The numbers associated with each branch represent statistical support values. The first value is the percentage of bootstrap in ML analysis; the second value is the posterior probability of the corresponding node in Bayesian inference. Only values above 75% for ML bootstrap and above 0.95 for Bayesian posterior probabilities are shown. Below these threshold values, the support values are indicated by a dash. Legends of the pictures: 1, *Fucus vesiculosus* L. (Fucales), herbarium; scale bar = 10 cm (© T. Silberfeld). 2, *Saccorhiza polyschides* (Lightfoot) Batters (Tilopteridales), drawing; scale bar = 10 cm (after Fritsch, 1945). 3, *Ralfsia fungiformis* (Gunnerus) Setchell *et* Gardner (Ralfsiales), herbarium; scale bar = 1 cm (© T. Silberfeld). 4, *Ascoseira mirabilis* Skottsberg (Ascoseirales), drawing; scale bar = 10 cm (after Delépine et al. 1987). 5, *Undaria pinnatifida* (Harvey) Suringar (Laminariales), herbarium; scale bar = 10 cm (© B. de Reviers). 6, *Colpomenia peregrina* Sauvageau (Ectocarpales), fresh specimen; scale bar = 2 cm (© B. de Reviers). 7, *Splachnidium rugosum* (L.) Greville (Scytothamnales), fresh specimen; scale bar = 5 cm (© Rob Anderson/algaebase.org). 8, *Bellotia eriophorum* Harvey (Sporochnales), herbarium; scale bar = 5 cm (© T. Silberfeld). 9, *Desmarestia ligulata* (Lightfoot) J.V. Lamouroux (Desmarestiales), herbarium; scale bar = 5 cm (© B. de Reviers). 10, *Halopteris filicina* (Grateloup) Kützing (Sphacelariales), herbarium; scale bar = 1 cm (© B. de Reviers). 11, *Syringoderma phinneyi* E.C. Henry *et* D.G. Müller (Syringodermatales), drawing; scale bar = 1 mm (after Henry and Müller, 1983). 12, *Dictyota dichotoma* (Hudson) J.V. Lamouroux (Dictyotales), herbarium; scale bar = 5 cm (© T. Silberfeld). The crustose species *Nemoderma tingitanum*, type of the Nemodermatales, has not been displayed.

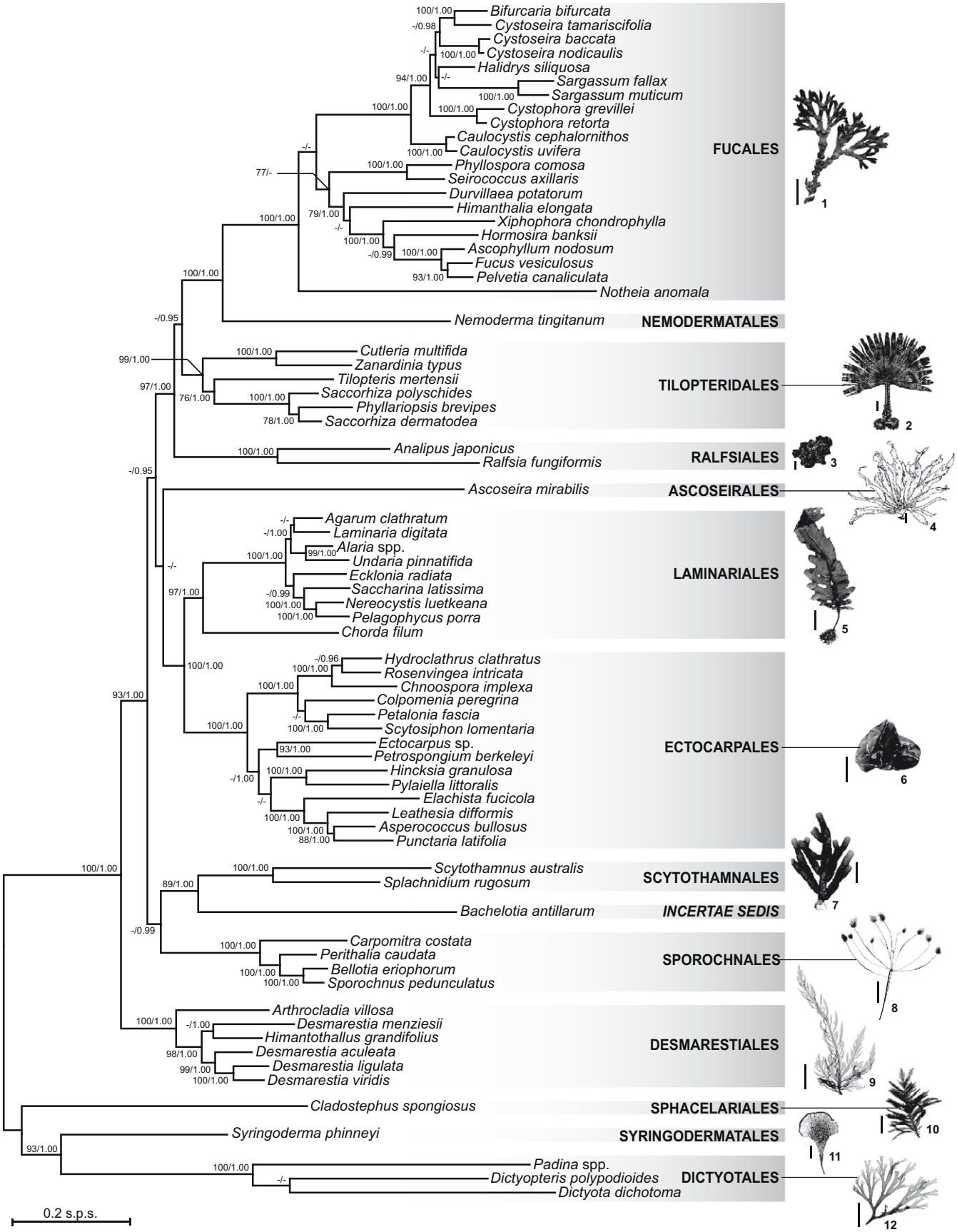
Bifurcaria bifurcata
Cystoseira tamariscifolia
Cystoseira baccata
Cystoseira nodicaulis
Halidrys siliquosa
Sargassum fallax
Sargassum muticum
Cystophora grevillei
Cystophora retorta
Caulocystis cephalornithos
Caulocystis uvifera
Phyllospora comosa
Seirococcus axillaris
Durvillaea potatorum
Himanthalia elongata
Xiphophora chondrophylla
Hormosira banksii
Ascophyllum nodosum
Fucus vesiculosus
Pelvetia canaliculata
Notheia anomala
FUCALES
Nemoderma tingitanum
NEMODERMATALES
Cutleria multifida
Zanardinia typus
Tilopteris mertensii
Saccorhiza polyschides
Phyllariopsis brevipes
Saccorhiza dermatodea
TILOPTERIDALES
Analipus japonicus
Ralfsia fungiformis
RALFSIALES
Ascoseira mirabilis
ASCOSEIRALES
Agarum clathratum
Laminaria digitata
Alaria spp.
Undaria pinnatifida
Ecklonia radiata
Saccharina latissima
Nereocystis luetkeana
Pelagophycus porra
Chorda filum
LAMINARIALES
Hydroclathrus clathratus
Rosenvingea intricata
Chnoospora implexa
Colpomenia peregrina
Petalonia fascia
Scytosiphon lomentaria
Ectocarpus sp.
Petrospongium berkeleyi
Hincksia granulosa
Pylaiella littoralis
Elachista fucicola
Leathesia difformis
Asperococcus bullosus
Punctaria latifolia
ECTOCARPALES
Scytothamnus australis
Splachnidium rugosum
SCYTOTHAMNALES
Bachelotia antillarum
INCERTAE SEDIS
Carpomitra costata
Perithalia caudata
Bellotia eriophorum
Sporochnus pedunculatus
SPOROCHNALES
Arthrocladia villosa
Desmarestia menziesii
Himantothallus grandifolius
Desmarestia aculeata
Desmarestia ligulata
Desmarestia viridis
DESMARESTIALES
Cladostephus spongiosus
SPHACELARIALES
Syringoderma phinneyi
SYRINGODERMATALES
Padina spp.
Dictyopteris polypodioides
Dictyota dichotoma
DICTYOTALES
0.2 s.p.s.
1
2
3
4
5
6
7
8
9
10
11
12

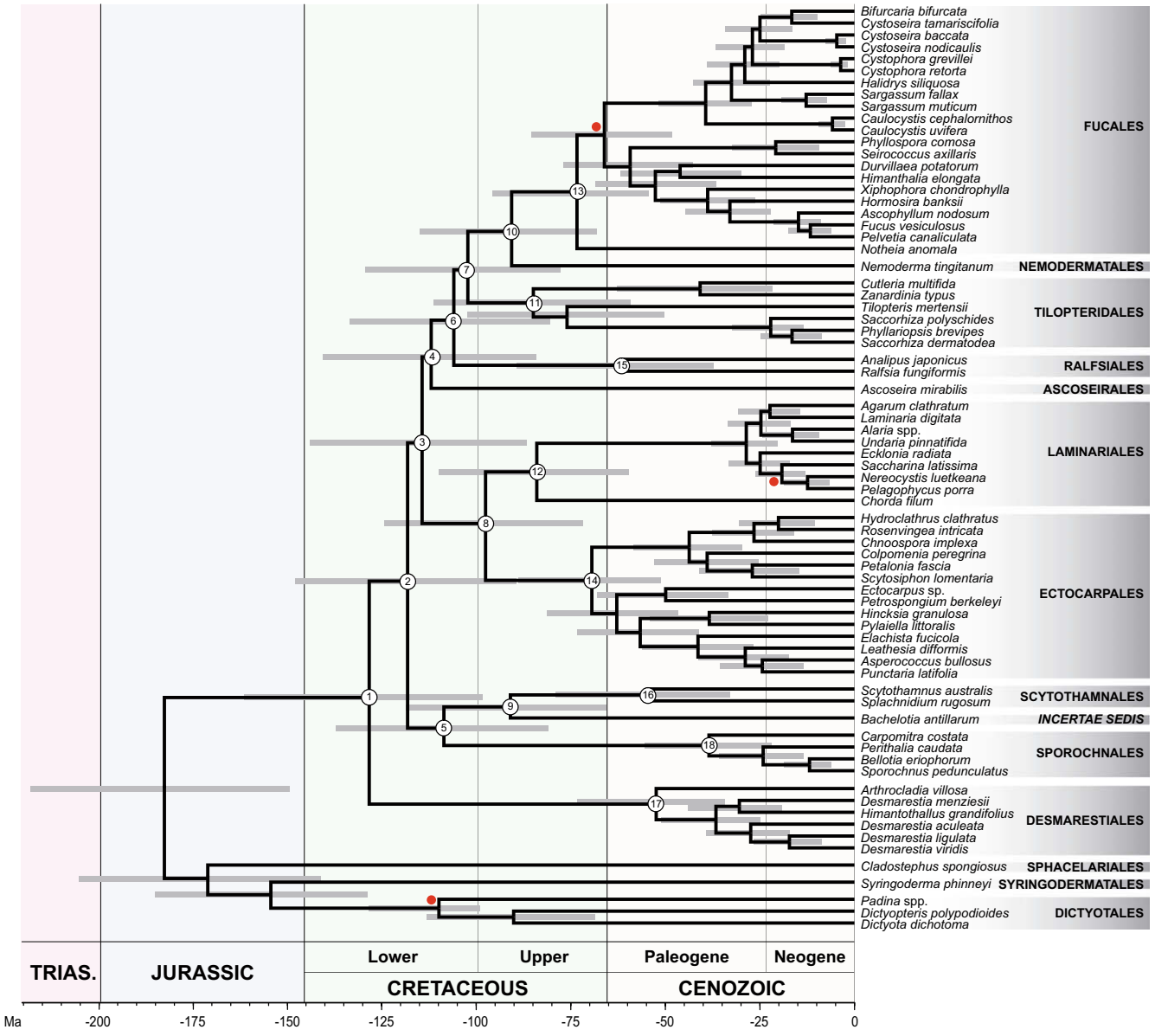

Fig. 2. Chronogram resulting from the Bayesian relaxed molecular clock analysis performed with BEAST (Drummond and Rambaut, 2007). The grey bars display the 95% HPD (highest probability density) interval of node ages. Details for nodes labelled with numbers are provided in Table 3. The red circles mark the three nodes that were time-constrained with fossils as described in text: the Sargassaceae and the (*Nereocystis–Pelagophycus*) lineage were constrained under a uniform prior with 13 Ma as lower boundary for their respective stem nodes, and the Dictyotales were constrained under a uniform prior with 13 Ma as lower boundary for their crown node. (For interpretation of the references to color in this figure legend, the reader is referred to the web version of this article.)

phyletic with strong to full support in both ML and BI analyses (BP = 100, PP = 1.00 for every order, except for Tilopteridales with BP = 98, and Laminariales with BP = 97).

Within the brown algal crown radiation, Desmarestiales is the first order to diverge, and it clustered as sister to all remaining orders with strong support (ML: BP = 93; BI: PP = 1.00). The next diverging lineage is a Sporochnales–Scytothamnales–*Bachelotia* clade that received strong support in BI and poor in ML (ML: BP < 75; PP = 0.99). Interestingly, the enigmatic *Bachelotia antillarum* was recovered as the sister lineage of the Scytothamnales with strong support (ML: BP = 89; BI: PP = 1.00). The Sporochnales–Scytothamnales–*Bachelotia* clade is sister to a clade encompassing all remaining orders, but support for this clade was moderate in BI and weak in ML (ML: BP < 75; BI: PP = 0.95). Nonetheless, this clade was recovered in all our analyses. With regard to the phylogenetic relationships among the remaining orders, two main clades could be observed: (1) an Ectocarpales–Laminariales clade with full support (MP: BP = 100; BI: PP = 1.00), and (2) a strongly supported clade encompassing the members of the Fucales, Nemodermatales, Tilopteridales and Ralfsiales (ML: BP = 97; BI: PP = 1.00). Within the latter lineage, the Mediterranean crustose genus *Nemoderma* was sister to the Fucales with full support (ML: BP = 100; BI: PP = 1.00). The Tilopteridales clustered with the Fucales–Nemodermatales clade with full support (ML: BP = 100, BI: PP = 1.00). Finally, the Ralfsiales were recovered as sister to the Fucales–Nemodermatales–Tilopteridales clade, though with poor to moderate support (ML: BP < 75; BI: PP = 0.95). The phylogenetic placement of the Ascoseirales, with the enigmatic Antarctic kelp-like *Ascoseira mirabilis* as the sole representative, remains unresolved, as it is impossible to state whether it allies with the Ectocarpales–Laminariales or the Fucales–Nemodermatales–Tilopteridales–Ralfsiales lineages.

Table 3
Bayesian posterior probability, mean age and 95% HPD interval for a selection of BACR nodes as displayed in Fig. 3.

Node	Description	Posterior probability	Mean age (Ma)	95% HPD interval (Ma)
1	Root of the BACR	1.00	128.9	98.7–162.0
2	–	1.00	118.7	89.5–148.4
3	–	0.88	114.8	87.0–144.6
4	–	0.46	112.4	84.5–141.1
5	Scyt–*Bach*–Spor clade	1.00	109.0	81.4–137.7
6	R–T–N–F clade	1.00	106.4	80.7–134.0
7	T–N–F clade	0.99	102.7	78.1–130.0
8	Laminariales–Ectocarpales clade	1.00	98.0	72.2–125.0
9	Scytothamnales–*Bachelotia*	1.00	91.4	65.9–119.0
10	Nemodermatales–Fucales clade	1.00	91.0	68.5–115.5
11	Tilopteridales	1.00	85.3	59.4–111.7
12	Laminariales	1.00	84.4	59.9–110.4
13	Fucales	1.00	73.7	54.6–96.0
14	Ectocarpales	1.00	69.7	51.4–89.3
15	Ralfsiales	1.00	62.0	37.5–89.7
16	Scytothamnales	1.00	54.9	33.1–79.4
17	Desmarestiales	1.00	52.7	34.4–73.7
18	Sporochnales	1.00	38.6	22.0–55.5

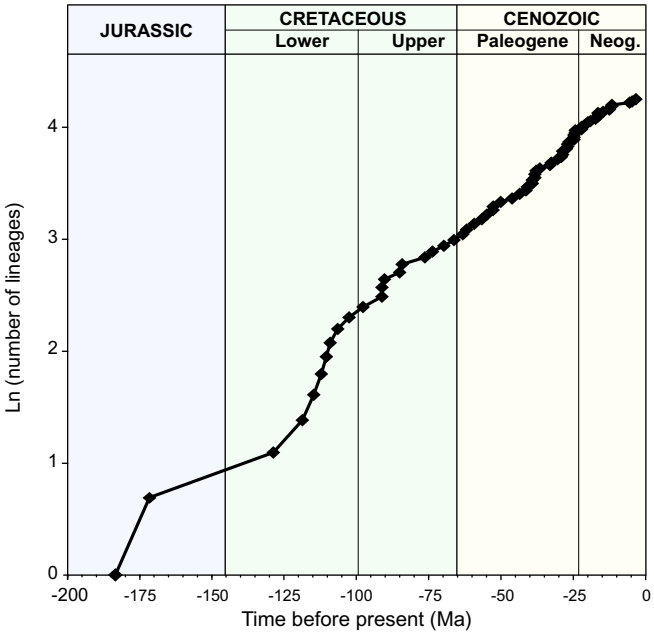

Fig. 3. Cumulative lineages-through-time (LTT) plot, built from the chronogram of Fig. 2, according to the method of Harvey et al. (1994). This diagram plots the cumulative natural logarithm of the number of occurring lineages against the mean age of their occurrence. A schematic time-scale has been displayed as background.

3.3. Time-calibrated phaeophycean phylogeny

The brown algal chronogram inferred from our data is presented in Fig. 2. For each labelled node, the inferred mean age and 95% highest density probability (95% HPD) intervals are provided in Table 3. As a consequence of the limited number of fossil constraints, most of which are fairly recent, the 95% HPD dramatically increase towards the root of the tree. However, when considering mean node ages, tentative conclusions about divergence times of the internal branches of the BACR are possible.

The first divergence of the brown algal crown radiation (node 1) would have occurred in the Lower Cretaceous (mean age 128.9 Ma) following a period of *ca* 50 Ma that did not produce any extant sister lineages to the BACR. From this point onwards, cladogenesis events seemingly occurred rapidly through time, with nodes 2–8 spanning a period of no more than 20 Ma until the end of Lower Cretaceous. The LTT curve (Fig. 3) displays a characteristic pattern with an increase in the slope around *ca* 125 Ma subsequent to a convex segment, technically known as an antisigmoidal curve (Harvey et al., 1994). Such a pattern is commonly taken to indicate a mass extinction episode followed by recovery of the diversity (Harvey et al., 1994). Consequently the relaxed clock analysis and the LTT plot suggest that the BACR represents a rapid diversification during the Lower Cretaceous.

3.4. Evolution of non-molecular characters

Fig. 4 shows the results of the ML ancestral state estimates for the six non-molecular characters that have dominated traditional order-level classifications of brown algae.

The heteromorphic life history seems to have evolved from isomorphic ancestry twice, once in Syringodermatales and once in the common ancestor of all BACR orders (Fig. 4A). Even though the root node received nearly equal probabilities for isomorphic and heteromorphic states, we consider the isomorphic condition more likely due to its presence in the earlier-diverging Ishigeales (Cho et al., 2004). Several reversals from a heteromorphic to an isomorphic condition are present within the BACR.

Regarding fertilization strategies, our analyses clearly suggest that the oogamous condition is ancestral for the BACR (Fig. 4B). Within the BACR, there is considerable uncertainty about ancestral conditions, with many nodes having similar probabilities for anisogamous and oogamous.

Terminal growth is likely to be the ancestral condition within the Phaeophyceae (Fig. 4C). It is present in Dictyotales, Sphacelariales and Syringodermatales as well as the earlier-branching brown algal lineages not included in our tree. It appears likely that intercalary growth has appeared in a common ancestor to the BACR and was subsequently lost in a few BACR lineages. The likelihood model suggests uncertainty about the presence of intercalary growth at the ancestral nodes relating the orders Ascoseirales, Ralfsiales, Tilopteridales, Nemodermatales and Fucales. Intercalary growth is subsequently regained in Durvillaeceae (Fucales), Tilopteridales and Ralfsiales.

Regarding the architecture of the macroscopic thallus, the ancestral state for the BACR is inferred to be a haplostichous structure (Fig. 4D). Since the early diverging lineages Discosporangiales and Ishigeales (not included in our study) are also haplostichous, it seems likely that the state at root of our tree should be considered haplostichous instead of polystichous as Fig. 4D suggests. The polystichous structure observed in the SSD clade is a synapomorphy of that clade yet not homologous to the polystichous structure that evolved in the Tilopteridales (Cutleriaceae and Tilopteridaceae). Within the BACR clade, multiple transitions from haplostichous to parenchymatous structure appear to have occurred, and perhaps vice versa, but the probabilities at the ancestral nodes leave doubt about the exact number of transitions.

The plastid characters exhibit simpler evolutionary patterns: the phaeophycean ancestor had several pyrenoid-less plastids per cell (Fig. 4E and F). Reductions to a single plastid occurred three times independently. A protruding pyrenoid has appeared only in the Ectocarpales (Rousseau and Reviers, 1999) whereas embedded plastids evolved at least twice.

4. Discussion

4.1. Longer alignments to resolve the BACR

Since the onset of brown algal molecular phylogenetics two decades ago, a massive polytomy near the base of the tree has left

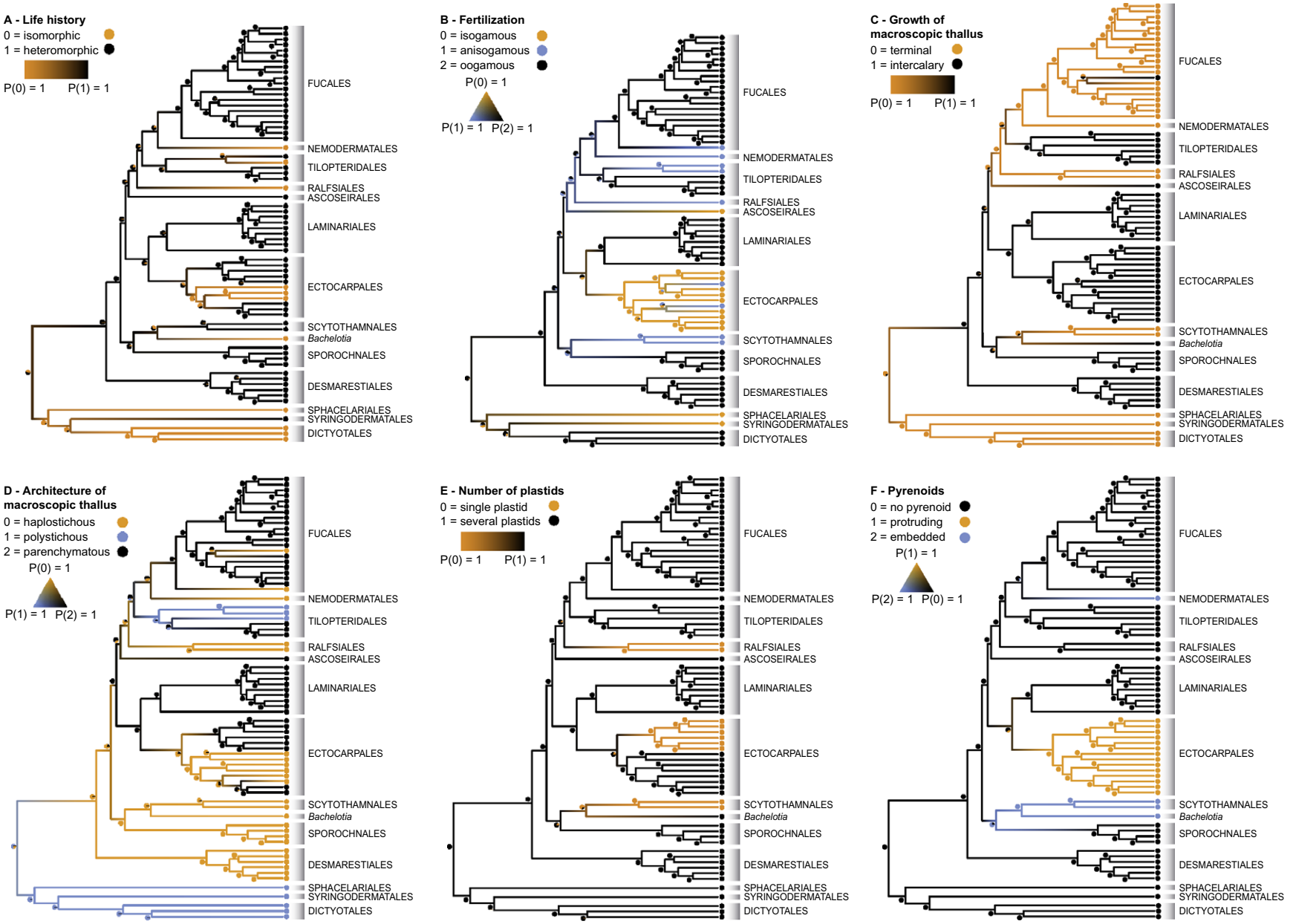

Fig. 4. Results of the ML-based ancestral character state estimation for six non-molecular characters on the chronogram topology of the Fig. 2. The six characters, traditionally considered as the most relevant in the field of brown algal systematics, are: A, type of life history; B, type of fertilization; C, growth of macroscopic thallus; D, architecture of macroscopic thallus; E, number of plastids; F, occurrence and structure of pyrenoid. The ML procedure provides a probabilistic assessment of the ancestral states; these probabilities are reflected in branch colors and pie diagrams at nodes. Each character state has been assigned a color and intermediate colors indicate uncertainty about the character state. For details, see the color caption associated with each tree.

researchers in doubt about the evolutionary history and systematics of the brown algae. The recent indications and speculations that the poor resolution in the BACR may be a consequence of a lack of informative data rather than the result of multiple, virtually instantaneous speciation events (Phillips et al., 2008a) have sparked new interest in resolving the BACR. Unpublished simulation studies (Braun *in* Phillips et al., 2008b) suggest that resolving the brown algal tree, and in particular the BACR, would need *ca* 20,000 nt of DNA data, which would correspond to 10–15 genes (Phillips et al., 2008b). By performing analyses on a combined data set of more than 10,000 nt including 10 markers from the three genomes, our study approaches this order of magnitude. As could be anticipated, our phylogenetic trees are well-resolved, confirming the ability of a multi-gene approach to improve the resolution of the brown algal crown.

The availability of five complete mitochondrial genome sequences (Oudot-Le Secq et al., 2001, 2002, 2006) facilitated primer design for the mitochondrial genes used in our study. To date, mitochondrial markers designed for phylogenetic purposes are scarce, and were mainly used at low taxonomic levels. For example, *cox*1 and *cox*3 were used to address species-level phylogenetic questions in kelp genera (Lane et al., 2007; Uwai et al., 2007). To our knowledge, only Lane et al. (2006) and Bittner et al. (2008) included mitochondrial markers in their data sets for phylogenetic studies within the orders Laminariales and Dictyotales. The inclusion of *cox*1, *cox*3, *nad*1, *nad*4 and *atp*9 in our dataset permits benchmarking the phylogenetic information content of these mitochondrial markers at the class level.

Although mitochondrial sequences included in our dataset exhibited higher substitution rates and stronger evidence for mutational saturation than plastid genes (see Section 3.1. and Supplementary Fig. S2), the mitochondrial genes also contained higher proportions of phylogenetically informative sites, even at the deep levels considered in this study. Our analyses were geared towards accommodating sites evolving at different rates, including fast sites. We inferred trees using likelihood-based models that explicitly take rate heterogeneity among sites into account. Specifically, the models we used allowed for the presence of a proportion of invariant sites (+I), and for the variant sites different gamma rate-categories were used (+Γ). The advantage of using these types of models to accommodate rate differences is that fast sites can be more safely included in analyses at deeper levels because they have little impact on the likelihood of deep relationships while still providing useful information about recent relationships (Yang, 2006). The benefits of the +I and +Γ model elements for phylogenetic inference, especially at deeper levels, have been documented (e.g. Gu et al., 1995). In addition, we geared our Bayesian analyses to accommodate rate differences among data partitions. It is well known that natural data partitions can vary in their evolutionary rates (e.g. different codon positions). We explicitly incorporated such overall rate variations among partitions into our analyses using the variable rate prior in MrBayes.

4.2. Inter-ordinal relationships

In the present work we provide good support across the brown algal tree of life by increasing the number of positions analysed. More importantly, our improved gene sampling provides stronger resolution of the BACR compared to previous work (Draisma et al., 2001; Rousseau et al., 2001; Phillips et al., 2008a). Our analyses confirm the position of the Desmarestiales as the earliest-diverging order of the BACR, the Laminariales–Ectocarpales relationship, and the position of Nemodermatales as sister to the Fucales. In addition, our analyses improved the resolution of other inter-ordinal nodes of the BACR, such as the close relationship between Scytothamnales and Sporochnales, the position of the enigmatic taxon *Bachelotia antillarum* as sister to the Scytothamnales, and complete resolution of the Ralfsiales–Tilopteridales–Nemodermatales–Fucales clade.

Despite this progress, some nodes within the BACR remain poorly resolved. First, the lineage clustering Laminariales, Ectocarpales, Ascoseirales, Ralfsiales, Tilopteridales, Nemodermatales and Fucales only receives poor support. Second, the position of *Ascoseira mirabilis* remains uncertain; this taxon may be either sister to the Fucales–Nemodermatales–Tilopteridales–Ralfsiales clade or the Laminariales–Ectocarpales clade. It is also worth noting that our tree shows very short internal branches connecting the component lineages of the BACR. So, despite the increase of resolution brought about by our sequencing effort, the BACR keeps displaying a pattern suggestive of rapid diversification.

4.3. Time-calibrated phylogeny

Two potential explanations for the radiative nature of the BACR are: (1) that it is a case of rapid cladogenesis and that the presently available data cannot resolve it (soft polytomy, Walsh et al., 1999) or (2) that it reflects truly simultaneous speciation events that cannot be resolved with any amount of data (hard polytomy, Walsh et al., 1999). We inferred and analysed a time-calibrated tree because a chronological framework can help us gain insight in such matters by giving us an estimate of how sudden the BACR diversification was. Furthermore, very little is known about the timeframe of brown algal evolution and our study is a first attempt at building a time-calibrated phylogeny based on Bayesian relaxed molecular clock analysis (Thorne et al., 1998; Drummond et al., 2006). Only a few studies (Medlin et al., 1997; Yoon et al., 2004; Berney and Pawlowski, 2006) have produced time-calibrated phylogenies including brown algae, but their focus was on broader evolutionary questions within the eucaryotes, and generally only allowed rough estimates of the age of the brown algae.

Before going into more detail about the timeframe of brown algal evolution suggested by our chronogram, we will focus our discussion on the rate of diversification spanning the BACR. Our chronogram shows the BACR as an episode spanning most of the Lower Cretaceous (*ca* 130–100 Ma). This relatively short, although not instantaneous, 30-Ma wide window of time over which the BACR lineages gradually diverged provides evidence that the brown algal crown radiation is not a hard polytomy, strengthening the case that the lack of resolution in various previous studies resulted from limited gene sampling. Phillips et al. (2008a) and the present study have shown that increasing alignment sizes resolves more of the BACR. We anticipate that additional gene sequencing will further resolve the BACR up to the point that the patterns of diversification are known without question. The antisigmoidal pattern displayed by the LTT plot is diagnostic for a period of increased diversification but not a single burst of diversification. Such patterns often emerge when, following an episode of mass extinction that occurs around the slope shift (in our case 130–110 Ma), diversity increases again during a recovery period (Crisp and Cook, 2009).

Interestingly, our chronogram recovers a possible correlation associating this pattern of extinction and recovery with massive basalt floods that resulted in the Large Igneous Province of Paraná, whose main volcanic paroxysm is dated 129–134 Ma (Peate, 1997). There is good evidence that volcanic episodes associated with extant basaltic trapps and large igneous provinces are linked to several mass extinctions, such as the Siberian Trapps and Deccan Trapps, associated to the Permian–Triassic (*ca* 250 Ma) and Cretaceous–Tertiary (*ca* 65 Ma) mass extinction crises, respectively (White and Saunders, 2005). One of the most common explanatory hypotheses to this link is a dramatic global warming and marine dysoxia episode due to a massive release of volcanic CO_2 in the

atmosphere (Wignall, 2001). Although to our knowledge there are no documented cases of extinction events contemporaneous to the Paraná igneous province, it is not beyond imagination that these climatic factors may have played a role in the extinction-recovery pattern suggested by our chronogram.

According to our time-calibrated phylogeny, most brown algal orders of the BACR have diversified in a timespan ranging through Upper Cretaceous and Paleogene. For instance, the diversification of Laminariales, Fucales and Ectocarpales is inferred to have begun around 84.4, 73.7 and 69.7 Ma, respectively (see Table 3 and Fig. 2). The oldest nodes in less diverse orders such as Desmarestiales and Sporochnales are only 52.7 Ma and 38.6 Ma old in our tree.

Previous molecular clock studies that included brown algae focused on eukaryotic algal diversification (Medlin et al., 1997; Yoon et al., 2004; Berney and Pawlowski, 2006), limiting the potential for comparison of our results. Medlin et al. (1997) produced a time-calibrated phylogeny that resulted in an estimate of the earliest origin of brown algae at *ca* 155 Ma. The extensive data set analysed by Berney and Pawlowski (2006) includes only *Fucus distichus* as a brown algal representative. In their time-calibrated phylogeny, the split between *Fucus distichus* and the tribophyte *Tribonema* is estimated to have occurred around 180 Ma (Lower Jurassic).

The identification of algal fossils suitable to elaborate a time-calibrated phylogeny is not a trivial task, even for groups for which an abundant and reliable fossil record is available (for an algal example, see Verbruggen et al., 2009). Brown algae have a particularly scarce fossil record (Draisma et al., 2003), and many of the fossils cannot even be confidently assigned to brown algae (Clayton 1984). The oldest supposedly brown algal fossils are *Dictyota*-like, dichotomously branched forms from the terminal Proterozoic (Xiao et al., 1998), Devonian (Fry and Banks, 1955; Hiller and Gess, 1996) and Carbo-Permian (Krings et al., 2007). Nevertheless, as pointed out by Krings et al. (2007), such dichotomous forms also occur in extant green algae, red algae, and even in land plants such as liverworts. Similarly, the seemingly bladder-like structures of the Silurian *Thalassocystis* (Taggart and Parker, 1976) are, in our opinion, insufficient to place it within the brown algae because very little detail is preserved and the available features are not very diagnostic. Even fossils described from younger deposits are often doubtful: e.g. the fossil described as *Cystoseira helvetica* in Heer (1877) from Eocene deposits of Switzerland is very fragmentary and only one sample is known. In the impossibility of further examination of Heer's original material, this fossil was not included.

We therefore, decided to only include three calibration points that are based on fossils showing clear evidence of a relationship to extant brown algal lineages. Two of the fossils in question are very young (Miocene) whereas the other dates back to the Early Cretaceous. It is evident that the fossil calibrations and the root prior we used have an impact on the quality of our chronogram. We thus, stress that this chronogram is to be regarded as a first attempt at a time-calibrated brown algal tree but that exact timeframe of brown algal evolution and the timing of the BACR will need confirmation from future molecular clock studies. Due to the absence of additional reliable brown algal fossils, this will probably require broadening the current sample of taxa to include related ochrophyte lineages with a more comprehensive fossil record (e.g. diatoms, dictyochophytes).

4.4. Character evolution

It has long been acknowledged that the high degree of morphological homoplasy was the main obstacle in creating natural classifications of brown algae (e.g. Draisma et al., 2001; Rousseau et al., 2001). Here, we used our improved brown algal phylogeny to reassess the evolutionary history of a set of morpho-anatomical characters that were considered important for brown algal classification and evaluate the amount of convergent morpho-anatomical evolution.

4.4.1. Reproductive features

The type of life history (Fig. 4A) and fertilization (Fig. 4B) display complex evolutionary patterns. A heteromorphic life history with microscopic gametophytes, as observed in Desmarestiales, Sporochnales, Scytothamnales and Laminariales, is likely to be ancestral for taxa of the BACR. As a consequence, the isomorphic life history observed in Ralfsiales, a few Tilopteridales (*Zanardinia* Zanardini and *Tilopteris* Kützing), and some Ectocarpalean lineages (e.g. Acinetosporaceae, e.g. the genera *Pylaiella* and *Hincksia*) appears to have resulted from independent reversions.

Regarding the fertilization strategy (Fig. 4B), the ML-based method resulted in uncertainty about the ancestral condition at several nodes of the BACR. Nonetheless, the oogamous ancestral state is recovered with high probability in the common ancestor of the BACR. At first sight this result may seem counter-intuitive, since a concept of unidirectional evolutionary progression from isogamy over anisogamy to oogamy has long been accepted (see for instance Wynne and Loiseaux, 1976; Clayton, 1988; Van Den Hoek et al., 1995). A series of models were built to explain the convergent evolution from isogamy to oogamy over anisogamy in the tree of Life (Parker et al., 1972; Bell, 1978; Bell, 1997; Dusenbery, 2002, among others). According to Bell (1997), large eggs are selected because they produce larger sporophytes, which in turn enhance dispersal of spores. We clearly found that a heteromorphic life history with dominant sporophytes, as observed in most of the BACR lineages, would have appeared from an ancestral isomorphic condition in a common ancestor to all BACR lineages (Fig. 4A). Assuming that gamete dimorphism and a heteromorphic life history evolve in parallel as suggested in Bell (1997), it appears less surprising to also retrieve the occurrence of oogamy in a common ancestor to all BACR lineages. Dusenbery (2002) speculated that gamete dimorphism is related to the production of sperm attractants (pheromones), which results in the selection of large female gametes with increased pheromonal target area and mating probability with small, motile swarmers. However, because the larger the gametes are, the fewer can be produced from a given biomass, gamete dimorphism will evolve only if the survival of zygotes increases disproportionately with their size (Parker et al., 1972; Bell, 1978, 1997). Some observations suggest that the evolution of oogamy may not be unidirectional. Basically, the persistence of flagella on the male gametes of all oogamous brown algae suggests that a fully functional genetic apparatus involved in flagellum formation is still present in their genome. Moreover the documented case of eggs bearing flagella in *Laminaria angustata* (Motomura and Sakai, 1987) confirms the notion that the loss of flagella in oocytes may be reversible.

However, our result should obviously be taken with caution. First, the inferred evolutionary scenario of gamete morphology depends on the taxon sampling and the tree topology and branch lengths. To further test this hypothesis, it would be necessary to consider a broader taxon sampling, including early diverging lineages (Ishigeales, Discosporangiales). The use of equal transition rates between states is a second major assumption of our analysis. Allowing different transition rates to occur may be more realistic from a biological point of view, but it has been shown that estimating six rate parameters instead of one with the same level of accuracy would require a considerably greater amount of data, and therefore often yields higher uncertainty about the parameter estimates and the inferred ancestral states (Mooers and Schluter, 1999; Pagel, 1999).

4.4.2. Macromorphological features

Regarding macroscopic thallus growth (Fig. 4C), it appears that growth by an intercalary meristem may have appeared in the ancestor of the BACR, and that it is a symplesiomorphy of the Desmarestiales, Sporochnales, Laminariales and Ectocarpales. The ancestral states are reconstructed with higher uncertainty at nodes connecting Ascoseirales, Ralfsiales, Tilopteridales, Nemodermatales and Fucales.

As pointed out by Phillips et al. (2008a), the Desmarestiales and the Sporochnales have long been considered to be closely related, mainly because they share trichothallic growth by a bidirectional intercalary meristem (Fritsch, 1945; Clayton, 1984). This traditional opinion even led some taxonomists to merge these taxa in a single order Desmarestiales (Russell and Fletcher, 1975) and the close relationship of these two orders was even confirmed in the early molecular work of Tan and Druehl (1996). However, in our analyses the Desmarestiales and the Sporochnales do not form a monophyletic lineage. As commented in Phillips et al. (2008a), the intercalary meristem observed in the Desmarestiales and the Sporochnales may also be homologous to the multifacial intercalary meristems (stipo-frondal zone) characteristic of the Laminariales and also observed in the Ascoseirales. Thus, with this hypothesis, the terminal growth characterizing the BACR orders Fucales, Nemodermatales, Ralfsiales and Scytothamnales probably results from homoplasic evolution. The observation that young seedlings of *Fucus* exhibit a hair resulting from an early trichothallic meristem (Fritsch, 1945) is consistent with this hypothesis.

The haplostichous thallus architecture (i.e. fundamentally made of filaments only growing by transversal cleavages) is likely to be the ancestral condition of the BACR (Fig. 4D) and is also observed in related classes such as Schizocladiophyceae (Kawai et al., 2003) and Phaeothamniophyceae (Bailey et al., 1998). A polystichous architecture (i.e. fundamentally made of filaments in which longitudinal cleavages also occur), can be anticipated to be a synapomorphy of the SSDO clade because early diverging brown algal orders outside our taxon sampling exhibit a haplostichous construction: for example the Discosporangiales (Kawai et al., 2007) and Ishigeales (Cho et al., 2004), as well as the more distant Schizocladiophyceae (Kawai et al., 2003) and Phaeothamniophyceae (Bailey et al., 1998). Within the BACR, a parenchymatous organization (i.e. produced by an initial cell or group of cells that undergo cleavages on all faces) is likely to have appeared in a common ancestor to Fucales, Nemodermatales, Tilopteridales, Ralfsiales, Ascoseirales, Laminariales and Ectocarpales from a haplostichous condition as displayed in Desmarestiales, Sporochnales and Scytothamnales. Subsequently the parenchymatous organization has probably reversed multiple times to a haplostichous (Ectocarpales, Ralfsiales) or polystichous (Tilopteridales Cutleriaceae and Tilopteridaceae) architecture. Describing the pattern in more detail is precarious due to uncertainties in the ancestral state reconstructions; e.g. it is impossible to state whether the parenchymatous organization of Fucales was secondarily gained, or acquired in an earlier intra-BACR ancestor.

4.4.3. Cytological features

Finally, plastid-related characters correspond much better with the phylogenetic framework, clearly showing less homoplasy (Fig. 4E and F). From an ancestor displaying the ancestral condition with several discoid, pyrenoid-free plastids per cell, reductions to a single plastid occurred in three lineages: the Ralfsiales, Scytothamnales and the Scytosiphonaceae within the Ectocarpales. Only the Ectocarpalean plastids have developed a single protruding pyrenoid (Rousseau and Reviers, 1999). Pyrenoids are also reported in members of the Scytothamnales–*Bachelotia* lineage. Moreover pyrenoids have recently been reported in the plastids of *Nemoderma tingitanum* (Nemodermatales) (Parente et al., 2000), although this observation has not been confirmed with ultrastructural observation. By all means they all have been acquired independently in these lineages.

It is worth focusing on the interesting case of the Scytothamnales–*Bachelotia* lineage. *Bachelotia* as well as the members of the Scytothamnales exhibit a stellate configuration of their plastidomes. The three genera of the Scytothamnales *sensu stricto* (*Scytothamnus* Hooker *et* Harvey, *Splachnidium* Greville and *Stereocladon* Hooker *et* Harvey) are characterized by a single lobate, star-shaped chloroplast with a large central pyrenoid embedded in the stroma (Peters and Clayton, 1998; Tanaka et al., 2007). *Bachelotia antillarum* exhibits several elongated chloroplasts with apical embedded pyrenoid, joined at their pyrenoids to form a stellate arrangement (Magne, 1976; Asensi et al., 1977; Uwai et al., 2005). This is of particular interest since the present study fully resolves the position of *Bachelotia antillarum*, as sister to the Scytothamnales. To date, the phylogenetic position of the species *Bachelotia antillarum* has always remained unresolved and/or poorly supported in all analyses previously performed (Rousseau et al., 2001; Uwai et al., 2005; Phillips et al., 2008a). This resulted in its uncertain ordinal assignment. It is beyond the scope of this paper to examine further ultrastructural characters likely to help building a consistent scenario of the evolution of the stellate plastidomes, all the more the remaining brown algal taxa featuring a stellate plastidome could not be included in our sampling: that is, the genus *Asterocladon* Müller, Parodi *et* Peters, closely related to Ectocarpales, and the genera *Asteronema* Delépine *et* Asensi and *Stereocladon* Hooker *et* Harvey (Müller and Parodi, 1994; Müller et al., 1998; Peters and Clayton, 1998; Uwai et al., 2005; Tanaka et al., 2007). Nevertheless, we suggest that *Bachelotia* should be merged within the Scytothamnales.

4.5. Concluding remarks

Our phylogenetic analyses of a 72 taxa by >10000 nt alignment of brown algae has allowed us to characterize the evolutionary nature of the "Brown Algal Crown Radiation" in more detail. First, regarding the possible effect of data quality and quantity on the resolution of the BACR, we showed that a substantial increase of the alignment size resolved a good amount of the relationships within the BACR. Nonetheless, several branches still did not obtain satisfactory support. Second, our application of a relaxed molecular clock showed that the BACR corresponds to an episode of accelerated cladogenesis during the Lower Cretaceous, resulting in several short, though not zero-length, internal branches. The *ca* 30 Ma period of evolutionary time over which the BACR lineages diverged from each other suggests that the BACR is a soft polytomy that could not previously be resolved due to alignment size limitations. This observation along with the fact that, through the history of brown algal phylogenetic studies, increasing amounts of data have contributed to provide more support in the BACR, suggests that a complete resolution of the BACR is not inconceivable.

Acknowledgments

We acknowledge Tristan Le Goff, Alan Millar, Kathy Miller, Richard Moe, Claude Payri, Akira Peters, Nathalie Simon and Nick Yee for their kind supply of silica-gel dried brown algal samples. We thank the Computational biology service unit of the Cornell University (http://cbsu.tc.cornell.edu/) for making available online their MrBayes and BEAST cluster facilities. Thomas Silberfeld is most grateful to Michaël Manuel (UPMC) for enlightening scientific discussions, Marie-Lilith Patou and Julien Lorion for their assistance with the molecular dating methods, Anna Plassart and Lucie Bittner for their undivided support. Heroen Verbruggen thanks Stefano Draisma and Steve LoDuca for sharing their insights and

opinions about brown algal fossils. The molecular work was undertaken at the "Service de Systématique Moléculaire" of the Muséum National d'Histoire Naturelle (UMS 2700); we are grateful to Annie Tillier, Josie Lambourdière and Céline Bonillo for their help and advice in the molecular lab. Finally we thank two anonymous referees for their thorough revisions and constructive criticism on a first version of the manuscript. This work was supported by the "Consortium National de Recherche en Génomique"; it is part of the agreement No. 2005/67 between the Genoscope and the Muséum National d'Histoire Naturelle on the project "Macrophylogeny of life" directed by Prof. Guillaume Lecointre. Thomas Silberfeld benefited of a grant from the French 'Ministère de l'enseignement supérieur et de la recherche'.

Appendix A. Supplementary data

Supplementary data associated with this article can be found, in the online version, at doi:10.1016/j.ympev.2010.04.020.

References

Akaike, H., 1974. A new look at the statistical model identification. IEEE Trans. Automat. Contr. 19, 716–723.

Asensi, A., Delépine, R., Gugliemi, G., 1977. Nouvelles observations sur l'ultrastructure du plastidome des Phéophycées. Bull. Soc. Phycol. Fr. 22, 192–205.

Bailey, J.C., Bidigare, R.R., Christensen, S.J., Andersen, R.A., 1998. Phaeothamniophyceae *classis nova*: a new lineage of Chromophytes based upon photosynthetic pigments, *rbc*L sequence analysis and ultrastructure. Protist 149, 245–263.

Bell, G., 1978. The evolution of anisogamy. J. Theor. Biol. 73, 247–270.

Bell, G., 1997. The evolution of the life cycle of brown seaweeds. Biol. J. Linn. Soc. 60, 21–28.

Berney, C., Pawlowski, J., 2006. A molecular time-scale for eukaryote evolution recalibrated with the continuous microfossil record. Proc. R. Soc. B 273, 1867–1872.

Bittner, L., Payri, C.E., Couloux, A., Cruaud, C., de Reviers, B., Rousseau, F., 2008. Molecular phylogeny of the Dictyotales and their position within the brown algae, based on nuclear, plastidial and mitochondrial sequence data. Mol. Phylogenet. Evol. 49, 211–226.

Charrier, B., Coelho, S.M., Le Bail, A., Tonon, T., Michel, G., Potin, P., Kloareg, B., Boyen, C., Peters, A.F., Cock, J.M., 2008. Development and physiology of the brown alga *Ectocarpus siliculosus*: two centuries of research. New Phytol. 177, 319–332.

Cho, G.Y., Lee, S.H., Boo, S.M., 2004. A new brown algal order, Ishigeales (Phaeophyceae), established on the basis of plastid protein-coding *rbc*L, *psa*A, and *psb*A region comparisons. J. Phycol. 40, 921–936.

Cho, G.Y., Rousseau, F., de Reviers, B., Boo, S.M., 2006. Phylogenetic relationships within the Fucales (Phaeophyceae) assessed by the photosystem I coding *psa*A sequences. Phycologia 45, 512–519.

Clayton, M.N., 1984. Evolution of the Phaeophyta with particular reference to the Fucales. In: Round, F.E., Chapman, D.J. (Eds.), Progress in Phycological Research, vol. 3. Biopress Ltd., Bristol, pp. 12–46.

Clayton, M.N., 1988. Evolution and life histories of brown algae. Bot. Mar. 31, 379–387.

Crisp, M.D., Cook, L.G., 2009. Explosive radiation or cryptic mass extinction? Interpreting signatures in molecular phylogenies. Evolution 63, 2257–2265.

Delépine, R., Asensi, A., Etcheverry, H., Antezana, T., 1987. Seaweeds. In: Fisher, W., Hureau, J.-C. (Eds.), FAO species identification sheets for fishery purposes. Southern Ocean (Fishing areas 48, 58 and 88) (CCAMLR Convention Area), vol. 1. FAO, Rome, pp. 1–69.

Draisma, S.G.A., Prud'homme van Reine, W.F., 2001. Onslowiaceae fam. nov. (Phaeophyceae). J. Phycol. 37, 647–649.

Draisma, S.G.A., Prud'Homme van Reine, W.F., Stam, W.T., Olsen, J.L., 2001. A reassessment of phylogenetic relationships within the Phaeophyceae based on RUBISCO large subunit and ribosomal DNA sequences. J. Phycol. 37, 586–603.

Draisma, S.G.A., Peters, A.F., Fletcher, R.L., 2003. Evolution of the Phaeophyceae: effects of the molecular age on brown algal systematics. In: Norton, T. (Ed.), Out of the Past. British Phycological Society, Liverpool, pp. 87–102.

Drummond, A.J., Ho, S.Y.W., Phillips, M.J., Rambaut, A., 2006. Relaxed phylogenetics and dating with confidence. PLoS Biol. 4, e88. doi:10.1371/journal.pbio.0040088.

Drummond, A.J., Rambaut, A., 2007. BEAST: Bayesian evolutionary analysis by sampling trees. BMC Evol. Biol. 7, 214–221.

Dusenbery, D.B., 2002. Ecological models explaining the success of distinctive sperm and eggs (oogamy). J. Theor. Biol. 219, 1–7.

Farris, J.S., Källersjö, M., Kluge, A.G., Bult, C., 1994. Testing significance of incongruence. Cladistics 10, 315–319.

Felsenstein, J., 1985. Confidence limits on phylogenies: an approach using the bootstrap. Evolution 39, 783–791.

Fritsch, F.E., 1945. The structure and reproduction of the algae, vol. 2. Cambridge University Press, Cambridge.

Fry, W.L., Banks, H.P., 1955. Three new genera of algae from the upper Devonian of New York. J. Paleontol. 29, 37–44.

Geuten, K., Massingham, T., Darius, P., Smets, E., Goldman, N., 2007. Experimental design criteria in phylogenetics: where to add taxa. Syst. Biol. 56, 609–622.

Gu, X., Fu, Y.X., Li, W.H., 1995. Maximum likelihood estimation of the heterogeneity of substitution rate among nucleotide sites. Mol. Biol. Evol. 12, 546–557.

Guiry, M.D., Guiry, G.M., 2010. *AlgaeBase*. World-wide electronic publication, National University of Ireland, Galway. <http://www.algaebase.org> accessed 9.05.2010.

Harvey, P.H., May, R.M., Nee, S., 1994. Phylogenies without fossils. Evolution 48, 523–529.

Heer, O., 1877. Flora fossilis Helvetia. Die vorweltliche Flora der Schweiz. In: Wurster, J. & Comp. (Ed.), Zürich.

Henry, E.C., Müller, D.G., 1983. Studies on the life history of *Syringoderma phinneyi* sp. nov. (Phaeophyceae). Phycologia 22, 387–393.

Hiller, N., Gess, R.W., 1996. Marine algal remains from the upper Devonian of South Africa. Rev. Palaeobot. Palynol. 91, 143–149.

Huelsenbeck, J.P., Rannala, B., 1997. Phylogenetic methods come of age: testing hypotheses in an evolutionary context. Science 276, 227–232.

Huelsenbeck, J.P., Ronquist, F., 2001. MrBAYES: Bayesian inference of phylogeny. Bioinformatics 17, 754–755.

Hurvich, C.M., Tsai, C.L., 1989. Regression and time series model selection in small samples. Biometrika 76, 297–307.

Kawai, H., Sasaki, H., 2004. Morphology, life history, and molecular phylogeny of *Stschapovia flagellaris* (Tilopteridales, Phaeophyceae) and the erection of the family Stschapoviaceae fam. nov. J. Phycol. 40, 1156–1169.

Kawai, H., Maeba, S., Sasaki, H., Okuda, K., Henry, E.C., 2003. *Schizocladia ischiensis:* a new filamentous marine Chromophyte belonging to a new class, Schizocladiophyceae. Protist 154, 211–228.

Kawai, H., Hanyuda, T., Draisma, S.G.A., Müller, D.G., 2007. Molecular phylogeny of *Discosporangium mesarthrocarpum* (Phaeophyceae) with a reinstatement of the order Discosporangiales. J. Phycol. 43, 186–194.

Krings, M., Klavins, S.D., Barthel, M., Lausberg, S., Serbet, R., Taylor, T.N., Taylor, E.L., 2007. *Perissothallus*, a new genus for Late Pennsylvanian–Early Permian noncalcareous algae conventionally assigned to *Schizopteris* (aphleboid foliage). Bot. J. Linn. Soc. 153, 477–488.

Lane, C.E., Mayes, C., Druehl, L., Saunders, G.W., 2006. A multi-gene molecular investigation of the kelp (Laminariales, Phaeophyceae) resolves competing phylogenetic hypotheses and supports substantial taxonomic re-organization. J. Phycol. 42, 493–512.

Lane, C.E., Lindstrom, S.C., Saunders, G.W., 2007. A molecular assessment of northeast Pacific *Alaria* species (Laminariales, Phaeophyceae) with reference to the utility of DNA barcoding. Mol. Phylogenet. Evol. 44, 634–648.

Lee, M.S.Y., Hugall, A.F., 2003. Partitioned likelihood support and the evaluation of data set conflict. Syst. Biol. 52, 15–22.

Leigh, J.W., Susko, E., Baumgartner, M., Roger, A.J., 2008. Testing congruence in phylogenomic analysis. Syst. Biol. 57, 104–115.

Magne, F., 1976. Quelques caractères cytologiques du *Bachelotia antillarum* (Phéophycées, Ectocarpales). Phycologia 15, 309–319.

Medlin, L.K., Kooistra, W.H.C.F., Potter, D., Saunders, G.W., Andersen, R.A., 1997. Phylogenetic relationships of the 'golden algae' (haptophytes, heterokont chromophytes) and their plastids. Plant Syst. Evol. 11 (Suppl.), 187–219.

Motomura, T., Sakai, Y., 1987. The occurrence of flagellated eggs in *Laminaria angustata* (Phaeophyceae, Laminariales). J. Phycol. 24, 282–285.

Mooers, A.Ø., Schluter, D., 1999. Reconstructing ancestor states with maximum likelihood: support for one- and two-rate models. Syst. Biol. 48, 623–633.

Müller, D.G., Parodi, E., 1994. Asteronema rhodochortonoides nov. comb. (Ectocarpales, Phaeophyceae)–a newly recognized taxon with stellate chloroplast arrangement. Phycologia 33, 471–474.

Müller, D.G., Parodi, E., Peters, A.F., 1998. *Asterocladon lobatum* gen. et sp. nov., a new brown alga with stellate chloroplast arrangement, and its systematic position judged from nuclear rDNA sequences. Phycologia 37, 425–432.

Oudot-Le Secq, M.P., Fontaine, J.-M., Rousvoal, S., Kloareg, B., Loiseaux-De Goër, S., 2001. The complete sequence of a brown algal mitochondrial genome, the Ectocarpale *Pylaiella littoralis* (L.) Kjellm. J. Mol. Evol. 53, 80–88.

Oudot-Le Secq, M.P., Kloareg, B., Loiseaux-De Goër, S., 2002. The mitochondrial genome of the brown alga *Laminaria digitata*: a comparative analysis. Eur. J. Phycol. 37, 163–172.

Oudot-Le Secq, M.P., Loiseaux-De Goër, S., Stam, W.T., Olsen, J.L., 2006. Complete mitochondrial genomes of the three brown algae (Heterokonta: Phaeophyceae) *Dictyota dichotoma*, *Fucus vesiculosus* and *Desmarestia viridis*. Curr. Genet. 42, 47–58.

Pagel, M., 1999. The maximum likelihood approach to reconstructing ancestral character states of discrete characters on phylogenies. Syst. Biol. 48, 612–622.

Pagel, M., Meade, A., 2006. BayesTraits. Available from: <http://www.evolution.rdg.ac.uk/BayesTraits.html>.

Parente, M.I., Fletcher, R.L., Neto, A.I., 2000. New records of brown algae (Phaeophyta) from the Azores. Hydrobiologia 440, 153–157.

Parker, B.C., Dawson, E.Y., 1965. Non-calcareous marine algae from California Miocene deposits. Nova Hedwigia 10, 273–295.

Parker, G.A., Baker, R.R., Smith, V.G.F., 1972. The origin and evolution of gamete dimorphism and the male–female phenomenon. J. Theor. Biol. 36, 529–553.

Peate, D.W., 1997. The Paraná-Etendeka Province. In: Mahoney, J.J., Coffin, M.F., (Eds.). Large Igneous Provinces: Continental, Oceanic, and Planetary Flood Volcanism. Geophysical Monographic Series, vol. 1. Washington, DC, pp. 217–245.

Peters, A.F., Clayton, M.N., 1998. Molecular and morphological investigations of three brown algae genera with stellate plastids: evidence for Scytothamnales ord. nov. (Phaeophyceae). Phycologia 37, 106–113.

Peters, A.F., Ramírez, M.E., 2001. Molecular phylogeny of small brown algae, with special reference to the systematic position of *Caepidium antarcticum* (Adenocystaceae, Ectocarpales). Cryptogamie, Algol. 22, 187–200.

Phillips, N., Burrowes, R., Rousseau, F., de Reviers, B., Saunders, G.W., 2008a. Resolving evolutionary relationships among the brown algae using chloroplast and nuclear genes. J. Phycol. 44, 394–405.

Phillips, N., Calhoun, S., Moustafa, A., Bhattacharya, D., Braun, E.L., 2008b. Genomic insights into evolutionary relationships among heterokont lineages emphasizing the Phaeophyceae. J. Phycol. 44, 15–18.

Rajanikanth, A., 1989. A fossil marine brown alga from the Gangapur formation, Pranhita–Godavari graben. Curr. Sci. India 58, 78–80.

Rambaut, A., Drummond, A.J., 2009. Tracer. Available from: <http://beast.bio.ed.ac.uk/tracer>.

de Reviers, B., Rousseau, F., 1999. Towards a new classification of the brown algae. In: Round, F.E., Chapman, D.J. (Eds.), Progress in Phycology Research, vol. 13. Biopress Ltd., Bristol, pp. 107–201.

de Reviers, B., Rousseau, F., Draisma, S.G.A., 2007. Classification of brown algae from past to present and current challenges. In: Brodie, J., Lewis, J. (Eds.), Unravelling the Algae – The Past, Present and Future of Algal Molecular Systematics. Systematics Association (Publ.), London, pp. 267–284.

Rodriguez, F., Oliver, J.L., Marin, A., Medina, J.R., 1990. The general stochastic model of nucleotide substitution. J. Theor. Biol. 142, 485–501.

Ronquist, F., Huelsenbeck, J.P., 2003. MRBAYES 3: Bayesian phylogenetic inference under mixed models. Bioinformatics 19, 1572–1574.

Rousseau, F., de Reviers, B., 1999. Circumscription of the order Ectocarpales: bibliographical synthesis and molecular evidence. Cryptogamie, Algol. 20, 5–18.

Rousseau, F., Burrowes, R., Peters, A.F., Kuhlenkamp, R., de Reviers, B., 2001. A comprehensive phylogeny of the Phaeophyceae based on nrDNA sequences resolves the earliest divergences. C.R. Acad. Sci. Paris, Série 3, Sci. Vie/Life Sci. 324, 305–319.

Russell, G., Fletcher, R.L., 1975. A numerical taxonomic study of the British Phaeophyta. J. Mar. Biol. Assoc. UK 55, 763–783.

Sanders, K.L., Lee, M.S.Y., 2007. Evaluating molecular clock calibrations using Bayesian analyses with soft and hard bounds. Biol. Lett. 3, 275–279.

Sasaki, H., Flores-Moya, A., Henry, E.C., Müller, D.G., Kawai, H., 2001. Molecular phylogeny of Phyllariaceae, Halosiphonaceae and Tilopteridales (Phaeophyceae). Phycologia 40, 123–134.

Schwarz, G.E., 1978. Estimating the dimension of a model. Ann. Stat. 6, 461–464.

Snirc, A., Silberfeld, T., Bonnet, J., Tillier, A., Tuffet, S., Sun, J.-S., 2010. Optimization of DNA extraction from brown algae (Phaeophyceae) based on a commercial kit. J. Phycol. 46. doi: 10.1111/j.1529-8817.2010.00817.x.

Stamatakis, A., 2006. RA×ML-VI-HPC: maximum likelihood-based phylogenetic analyses with thousands of taxa and mixed models. Bioinformatics 22, 2688–2690.

Swofford, D.L., 1999. PAUP*. Phylogenetic Analyses Using Parsimony (*and other methods), version 4.0b10PPC. Sinauer Associates, Sunderland.

Taggart, R.E., Parker, L.R., 1976. A new fossil alga from the Silurian of Michigan. Am. J. Bot. 63, 1390–1392.

Tamura, K., Dudley, J., Nei, M., Kumar, S., 2007. MEGA4: Molecular Evolutionary Genetics Analysis (MEGA) software version 4.0. Mol. Biol. Evol. 24, 1596–1599.

Tan, I.H., Druehl, L.D., 1993. Phylogeny of the Northeast Pacific brown algal (Phaeophycean) orders as inferred from 18S rRNA gene sequences. Hydrobiologia 260 (261), 699–704.

Tan, I.H., Druehl, L.D., 1994. A molecular analysis of *Analipus* and *Ralfsia* (Phaeophyceae) suggests the order Ectocarpales is polyphyletic. J. Phycol. 30, 721–729.

Tan, I.H., Druehl, L.D., 1996. A ribosomal DNA phylogeny supports the close evolutionary relationships among the Sporochnales, Desmarestiales, and Laminariales (Phaeophyceae). J. Phycol. 32, 112–118.

Tanaka, A., Nagasato, C., Uwai, S., Motomura, T., Kawai, H., 2007. Re-examination of ultrastructure of the stellate chloroplast organization in brown algae: structure and development of pyrenoids. Phycol. Res. 55, 203–213.

Thorne, J.L., Kishino, H., Painter, I.S., 1998. Estimating the rate of evolution of the rate of molecular evolution. Mol. Biol. Evol. 15, 1647–1657.

Thomson, R., Shaffer, H.B., 2010. Rapid progress on the vertebrate tree of life. BMC Biol. 8, 19.

Uwai, S., Nagasato, C., Motomura, T., Kogame, K., 2005. Life history and molecular phylogenetic relationships of *Asterocladon interjectum* sp. nov. (Phaeophyceae). Eur. J. Phycol. 40, 179–194.

Uwai, S., Arai, S., Morita, T., Kawai, H., 2007. Genetic distinctness and phylogenetic relationships among *Undaria* species (Laminariales, Phaeophyceae) based on mitochondrial *cox*3 gene sequences. Phycol. Res. 55, 263–271.

Van den Hoek, C., Mann, D.G., Jahns, H.M., 1995. Algae: An Introduction to Phycology. Cambridge University Press, Cambridge.

Verbruggen, H., 2010. TreeGradients. Available from: <http://www.phycoweb.net>.

Verbruggen, H., Ashworth, M., LoDuca, S.T., Vlaeminck, C., Cocquyt, E., Sauvage, T., Zechman, F.W., Littler, D.S., Littler, M.M., Leliaert, F., De Clerck, O., 2009. A multi-locus time-calibrated phylogeny of the siphonous green algae. Mol. Phylogenet. Evol. 50, 642–653.

Walsh, H.E., Kidd, M.G., Moum, T., Friesen, V.L., 1999. Polytomies and the power of phylogenetic inference. Evolution 53, 932–937.

White, R.V., Saunders, A.D., 2005. Volcanism, impact and mass extinctions: incredible or credible coincidences? Lithos 79, 299–316.

Wignall, P.B., 2001. Large igneous provinces and mass extinctions. Earth Sci. Rev. 53, 1–33.

Wynne, M.J., Loiseaux, S., 1976. Recent advances in life history studies of the Phaeophyceae. Phycologia 15, 435–452.

Xiao, S.H., Knoll, A.H., Yuan, X.L., 1998. Morphological reconstruction of *Miaohephyton bifurcatum*, a possible brown alga from the Neoproterozoic Doushantuo Formation, South China. J. Paleontol. 72, 1072–1086.

Yang, Z., 2006. Computational molecular evolution. Oxford University Press. p. 321.

Yoon, H.S., Lee, J.Y., Boo, S.M., Bhattacharya, D., 2001. Phylogeny of Alariaceae, Laminariaceae and Lessoniaceae (Phaeophyceae) based on plastid-encoded RuBisCo spacer and nuclear-encoded ITS sequence comparisons. Mol. Phylogenet. Evol. 21, 231–243.

Yoon, H.S., Hackett, J.D., Ciniglia, C., Pinto, G., Bhattacharya, D., 2004. A molecular timeline for the origin of photosynthetic Eucaryotes. Mol. Biol. Evol. 21, 809–818.